REPORT NO. DOT/MTB/OHMR-80/2

PERFORMANCE OF PLASTIC PACKAGING FOR HAZARDOUS MATERIALS TRANSPORTATION

PART V. MECHANICAL PROPERTIES

JOHN M. CRISSMAN, LOUIS J. ZAPAS, AND
GORDON M. MARTIN

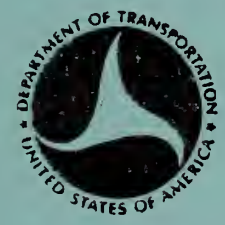

DECEMBER 1979
FINAL REPORT

Prepared for

U.S. DEPARTMENT OF TRANSPORTATION
MATERIALS TRANSPORTATION BUREAU
OFFICE OF HAZARDOUS MATERIALS RESEARCH
WASHINGTON, D.C. 20590

Testing of An Oxygen Depletion Detecting Device for Unvented Gas Fueled Heaters

Esher R. Kweller
William Cuthrell

Product Performance Engineering Division
Center for Consumer Product Technology
National Engineering Laboratory
National Bureau of Standards
Washington, D.C. 20234

June 1978

Issued January 1979

Prepared for
Consumer Product Safety Commission

NOTICE

PREFACE

This report is Part V in a series prepared for the Department of Transportation, Office of Hazardous Materials Research under Research Contract No. DoT AS-50074. Parts I and III were concerned with mechanical properties aspects of the performance of large shipping containers used for the transport of hazardous materials. Parts II and IV dealt with permeation aspects. Part V addresses the problems of stress-cracking in polyethylene and mechanical properties aspects of crosslinkable polyethylenes for rotational molding used in the manufacture of large shipping containers.

The authors wish to acknowledge the assistance and cooperation of the Office of Hazardous Materials Research Staff, in particular Mr. Mario Gigliotti. We are also indebted to Mr. Paul Campbell of the Phillips Chemical Company for providing us with sample materials.

TABLE OF CONTENTS

LIST OF TABLES

LIST OF FIGURES

1. Introduction

This report is Part V in a series of reports prepared for the U. S. Department of Transportation Office of Hazardous Materials Research (DoT OHMR) under DoT Contract AS-50074. In fiscal 1976, the National Bureau of Standards (NBS) Polymer Science and Standards Division initiated studies in the area of mechanical and permeation properties of plastic materials used in the manufacture of large shipping containers for the transport of hazardous materials. The findings of these investigations prior to the current reporting period can be found in references [1-4]*.

The present report summarizes experimental work done in the area of mechanical properties carried out since the completion of Part III [3]. The effort has been directed primarily toward (1) a continuation of the studies initiated in Part III on the stress-crack resistance of polyethylene, and (2) an examination of different test methods for determining the degree of crosslinking in crosslinkable polyethylenes for rotational molding.

2. Environmental Stress Cracking in Polyethylene

Part III in this series of reports [3] dealt in its entirety with the subject of environmental stress cracking of ethylene plastics. The first section provided a discussion of current ASTM test methods for determining environmental stress-crack resistance of ethylene plastics [5]. The second section presented general background information on chemical and physical characteristics of polyethylene which influence stress-crack resistance. In the third section, experimental work initiated in our laboratory in the area of stress cracking in polyethylene was summarized. These studies were limited primarily to time to fail under conditions of static fatigue in uniaxial creep in both air and various chemical environments.

Section 2 of the present report describes additional experiments in which a variety of methods have been examined for determining stress-crack resistance under biaxial deformation histories. In the interest of continuity and ease of reading, we shall first briefly review a portion of the earlier-work on uniaxial creep contained in Part III. In several instances, figures contained there have been reproduced here as well in order to facilitate the discussion. We review these results in order to illustrate a number of important points regarding the failure behavior of polyethylenes in general. The same observations will carry over into the area of biaxial deformations to be discussed later. Throughout this current study, we shall continue to concentrate on the same two high density polyethylenes described in Part III. These two were chosen originally because of their widely different stress-crack behavior as based on technical information provided by the resin manufacturer. As determined by ASTM D1693 [5], Condition A, an F_{50} value of 15-20 hours is quoted for the linear polymer, while that for the ethylene-hexene copolymer is 450 hours.

2.1 Uniaxial Creep

Shown in Figure 2.1.1 are log time to fail versus applied stress (engineering stress) data for specimens of the linear polyethylene tested to failure in air at four different temperatures. By failure is meant either the time at which necking of the specimen occurred or the time at which the specimen fractured due to cracking. The tendency for the curves to bend down at the highest levels of stress is a result of internal heating of the specimen during the rapid creep. In principle, one would like to use data of this type in order to predict the long time uniaxial creep behavior (failure time) for times well in excess of those for which data were actually collected, for example times in excess of 10^8 seconds at 296K (23°C). The ideal situation is one in which the data obtained at several elevated temperatures can be superposed to some reference temperature by simply shifting the curves along the time axis. The shift factors can then be plotted versus reciprocal temperature,

*Numbers in square brackets refer to references found at the back of this report.

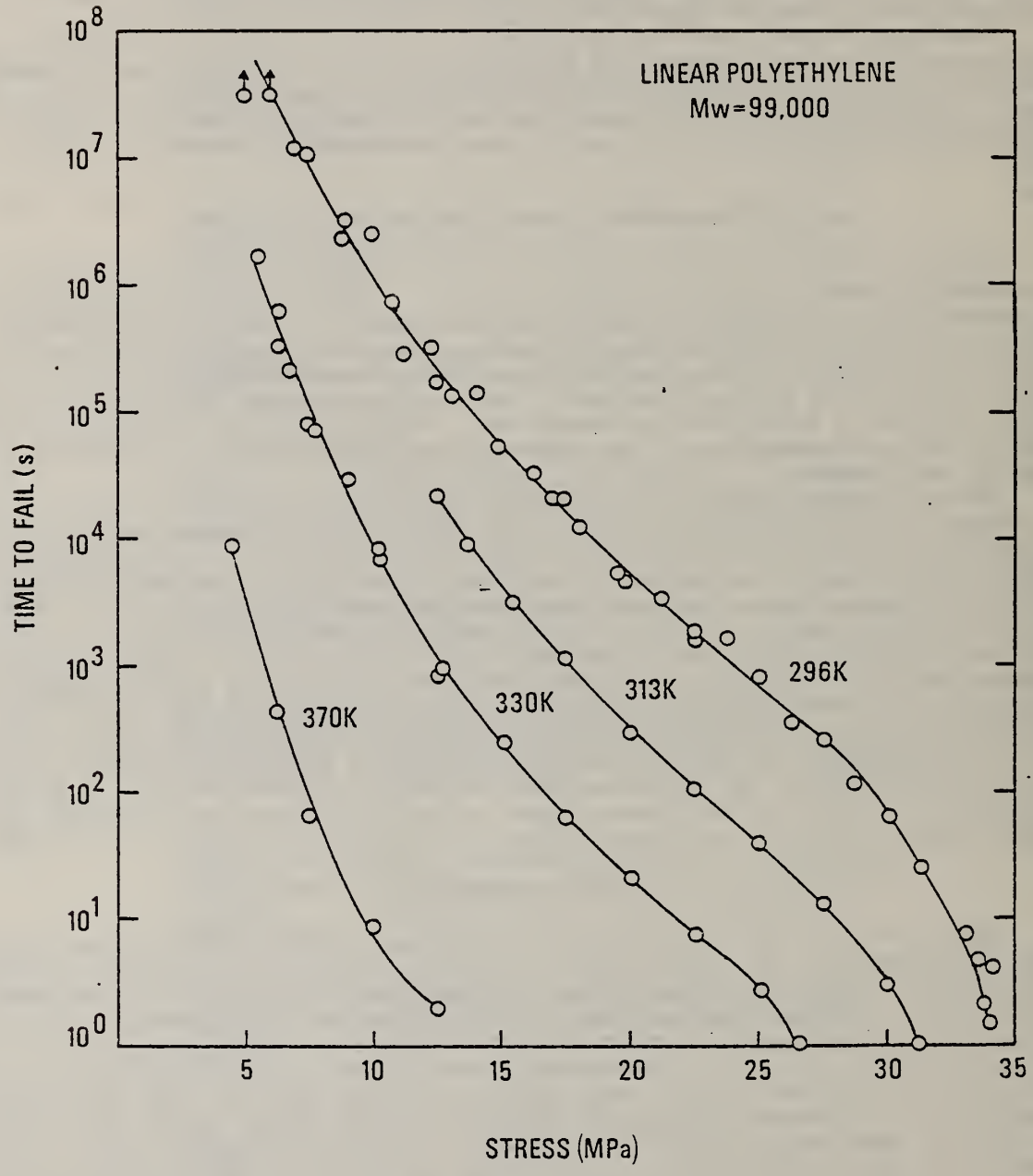

Figure 2.1.1 - Log time to fail versus applied stress in uniaxial creep for high density linear polyethylene (M_W = 99,000) in air.

and in the event that a straight line results, a temperature independent activation energy can be determined. This information can then be used to predict the time to fail for any other set of temperature and applied stress within the total range of temperatures and stresses investigated. Unfortunately, the data in Figure 2.1.1 cannot be superposed simply by a shift along the time axis (even when disregarding the bent down portions of the curves). One reason is that more than one failure mechanism is present, and importantly the activation energies for the different mechanisms are not the same. For stresses above about 15MPa the creep behavior becomes dominated by the viscoelastic properties of the polymer. In this region the specimen creeps to a sufficiently large strain that an instability occurs. By instability we mean the point beyond which the material can no longer undergo a homogeneous deformation. Beyond this point morphology or structure changes take place, for example void formation or localized yielding, and eventually necking of the specimen occurs. Based on a theoretical treatment by Zapas [6], Zapas and Crissman [7] have shown experimentally that for linear polyethylenes in the molecular weight range (M_W) from 100,000 to 200,000 the instability point for uniaxial extension occurs at a strain of about 10-12%. In fact, from creep data, it has been found possible to predict, well in advance of any visible evidence, the point in time at which necking will occur [7]. In terms of strain, necking generally occurs for linear polyethylene at about 25 to 30%, depending upon the magnitude of the stress and to some extent on the polymer type.

On the other hand, below about 12.5 MPa, the region of small applied stress, the specimens fail by cracking. In this regime, the specimen develops a crack which propagates through the specimen well before the global creep strain becomes sufficiently large to reach the point of instability. That this is true is illustrated by the creep behavior shown in Figure 2.1.2 for several of the same specimens for which time to fail data are presented in Figure 2.1.1. At large loads the creep characteristically becomes increasingly rapid with log time up to the point where necking occurs. In each case where the load was greater than about 14 MPa the creep strain at failure was greater than 12%. In the region of small applied loads the creep curves tend to flatten so that over a large percentage of the total time to failure the global strain remains nearly constant. In this event, the material more nearly approximates the behavior of an elastic material. It should be pointed out that (for linear polyethylenes) from the time that a crack first becomes visible until fracture occurs, the elapsed time is only a very small fraction of the total lifetime (time to failure). An interesting region is the one intermediate to the two extremes. For stresses between about 12.5 and 15 MPa (Figure 2.1.1) it cannot be anticipated which failure mode will prevail, and in some instances specimens have been observed to show both failure modes simultaneously.

Comparable time to fail versus applied stress data are shown for the ethylene-hexene copolymer in Figure 2.1.3. One feature to be noted here is that the curves are steeper than for the linear polymer. This behavior gives rise to the interesting result that at high stresses (> 14MPa) the copolymer fails earlier at a given stress than does the linear polymer, while at small stresses (< 14MPa) it has increasingly longer lifetime. Another important point regarding the copolymer is that the mechanism which leads to instability and eventual necking occurs even at very long times at room temperature (296K). We note that the only specimen of this material for which cracking was observed was one requiring 2.8 years to fail. As will be seen presently, this behavior will have considerable bearing on determining stress-crack resistance.

As a demonstration that the observed differences in behavior of the two polyethylenes is not simply one of a difference in molecular weight, we show in Figure 2.1.4 on log-log coordinates the time to fail behavior for three different samples of linear polyethylene. All three samples have very nearly the same number average molecular weight ($15\text{-}16 \times 10^4$) but different weight average molecular weights ($9.9 - 19.2 \times 10^4$). The sample having an M_W of 19.2×10^4 is nearly comparable to the ethylene-hexene copolymer for which $M_W = 21.1 \times 10^4$. Observe that at 296K all three polymers show essentially the same behavior. The small difference observable at the higher temperatures may reflect some difference in crystallinity between sample types.

Up to this point we have considered only the behavior in air, which for convenience will be regarded as the reference environment. It will be useful here to review briefly some of the earlier work on the uniaxial creep behavior of these same two polymers in the presence of stress-cracking agent or solvent. A description of the apparatus and procedures for carrying out the stress-cracking experiment in uniaxial creep have been given in Part III [3] and will not be repeated here. In the discussion which follows, the adverse environment was either a ten percent solution in distilled water of nonylphenoxypoly

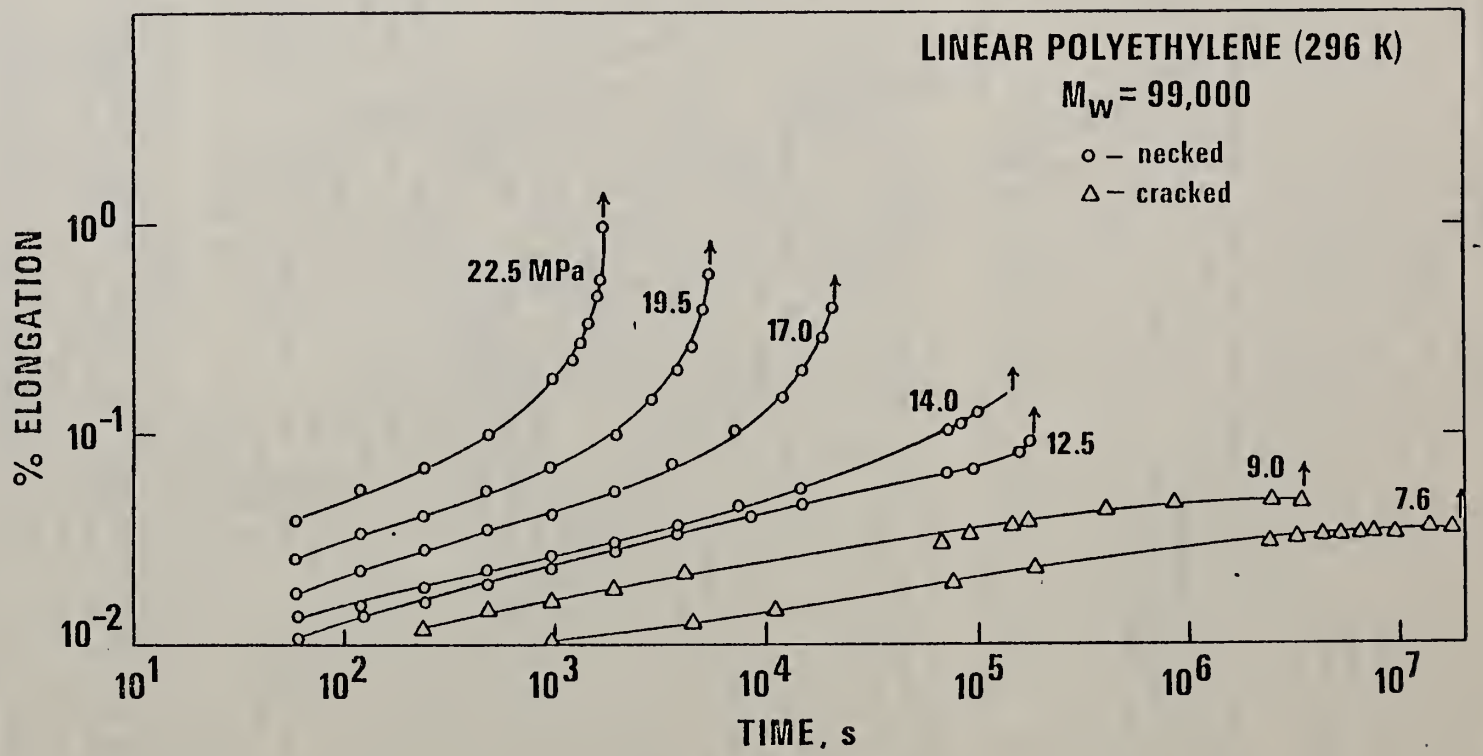

Figure 2.1.2 - Uniaxial creep behavior for specimens of high density linear polyethylene (M_W = 99,000) in air.

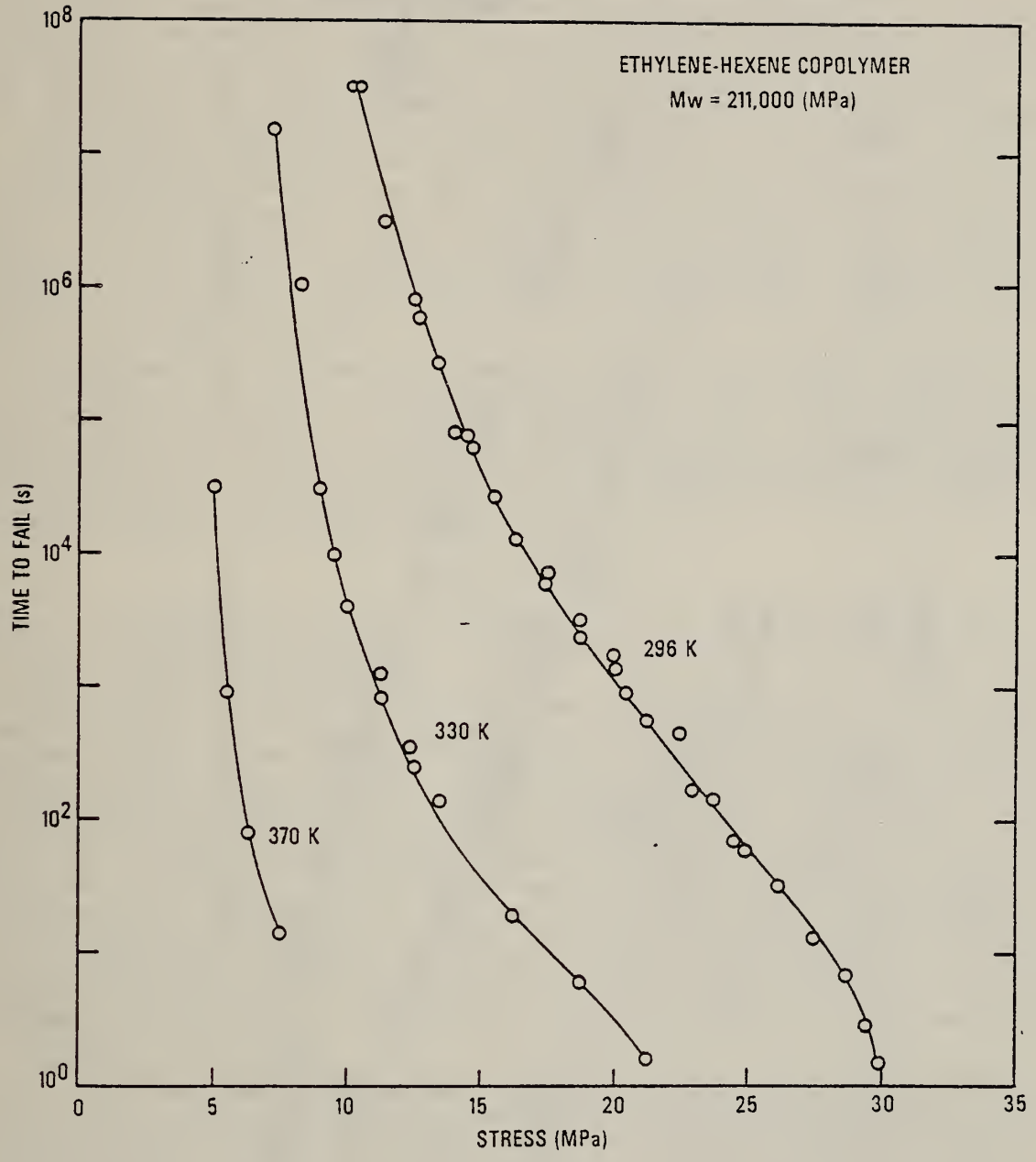

Figure 2.1.3 - Log time to fail versus applied stress in uniaxial creep for an ethylene-hexene copolymer (M_w = 211,000) in air.

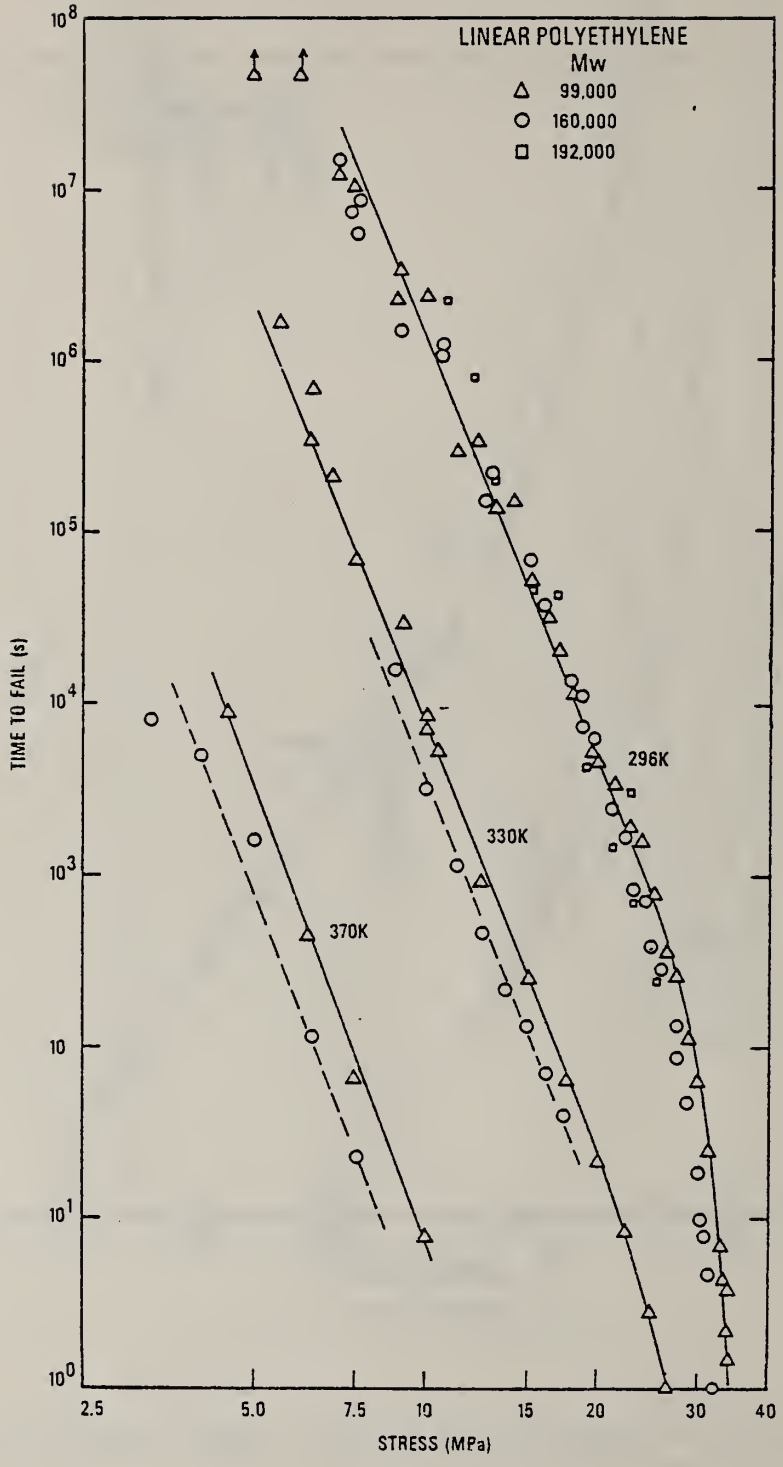

Figure 2.1.4 - Log time to fail versus log applied stress in uniaxial creep for three high density linear polyethylenes having different weight average molecular weights.

(ethyleneoxy)ethanol or the normal alkane, dodecane ($C_{12}H_{26}$). The first of these (hereafter referred to simply as stress-cracking agent) is regarded to be a surface active agent, whereas dodecane behaves as a swelling agent.

Results for the linear polymer in stress-cracking agent are shown in Figure 2.1.5 for two different temperatures. The solid lines represent the time to fail in air data from Figure 2.1.1 and the solid lines with triangles the behavior in stress-cracking agent. Above a certain stress, depending somewhat on the temperature, the curves for air and stress-cracking agent merge. Although data are not shown in the figure, at stresses higher than those for which data points are shown the behavior was the same in stress-cracking agent as in air. The region where the two curves come together corresponds to the point at which the failure mode changes from one of fracture by cracking to one of necking. Therefore, one conclusion to be drawn is that the failure behavior in the region associated with the instability is unaffected by the presence of this type of stress-cracking agent.

On the other hand, the failure mode involving fracture by cracking is influenced by the presence of the stress-cracking agent, and in such a way as to suggest that the action of the stress-cracking agent is one of a constant additive stress, in this case of about 2.2 MPa. It is an interesting feature that in air the time to fail curve is smooth overall, showing no abrupt change in character as the failure mode changes. On log-log coordinates (Figure 2.1.4) the behavior was very nearly linear over four or more decades in time. However, in the presence of the stress-cracking agent, the two failure mechanisms become quite distinct from one another.

As noted earlier, the creep strain at small stresses remains nearly constant over a high percentage of the total lifetime of the specimen, and the material behaves more in a manner similar to an elastic solid (strain independent of time). Such a behavior suggests that the mechanism associated with cracking can be treated in a way reminiscent of an inorganic glass. In an earlier work [8] we have shown that the time to fail behavior for the cracking mode can be represented rather well by the empirical relation developed some thirty years ago by Glathart and Preston [9] given by

$$\log t_B = A + B/\sigma, \qquad (1)$$

where t_B is the time to fracture, σ is the applied stress, and A and B are material constants. This analysis leads to an activation energy for the fracture process of about 124 kJ/mole (29.6 kcal/mole).

By way of contrast, the behavior of the same linear polyethylene in the n-paraffin, dodecane ($C_{12}H_{26}$), is presented in Figure 2.1.6. The dimensions used to calculate the stress are based on the unswollen specimen. In order to avoid time effects, the specimens were presoaked in the liquid for at least 16 hours prior to loading. Additional presoaking for longer periods had no appreciable influence on the final results. The behavior in solvent is markedly different than that in the stress-cracking agent. Whereas in stress-cracking agent, only the region corresponding to fracture by cracking is affected, in solvent the entire time to fail curve is shifted significantly. In solvent, triaxial stresses are introduced into the material due to swelling, and the effect appears to be comparable to that of an increase in temperature. In the case of amorphous polymers, it is known [10] that a swelling agent both shifts the relaxation times and lowers the moduli. If this same behavior holds true for semicrystalline polymers, one would then expect a shift along both the time and stress axis for superposition, as would appear to be the case from the results shown in Figure 2.1.6.

The behavior of the ethylene-hexene copolymer in stress-cracking agent is presented in Figure 2.1.7. The principle difference in behavior between copolymer and the linear polymer is that the point at which the time to fail in the stress-cracking agent deviates from the behavior in air occurs at longer times. This result is consistent with the remark made earlier that the failure associated with instability and necking extends out to much longer times for the copolymer than for the linear polymer. At 296K, quite long times are required before the influence of the stress-cracking agent becomes apparent. However, by raising the temperature to 330K (57°C) the deviation in behavior occurs at relatively short times.

One interesting result of this work can be seen by plotting the log time to fail in adverse environment versus the log time to fail in air, all data obtained at 330K, as is shown in Figure 2.1.8. The dashed line denotes behavior that does not deviate from that in air. The vertical distance from the dashed line can be interpreted as a measure of the reduction of the static fatigue life brought about by the presence of an adverse chemical environment. In stress-cracking agent the reduction in lifetime for the copolymer actually

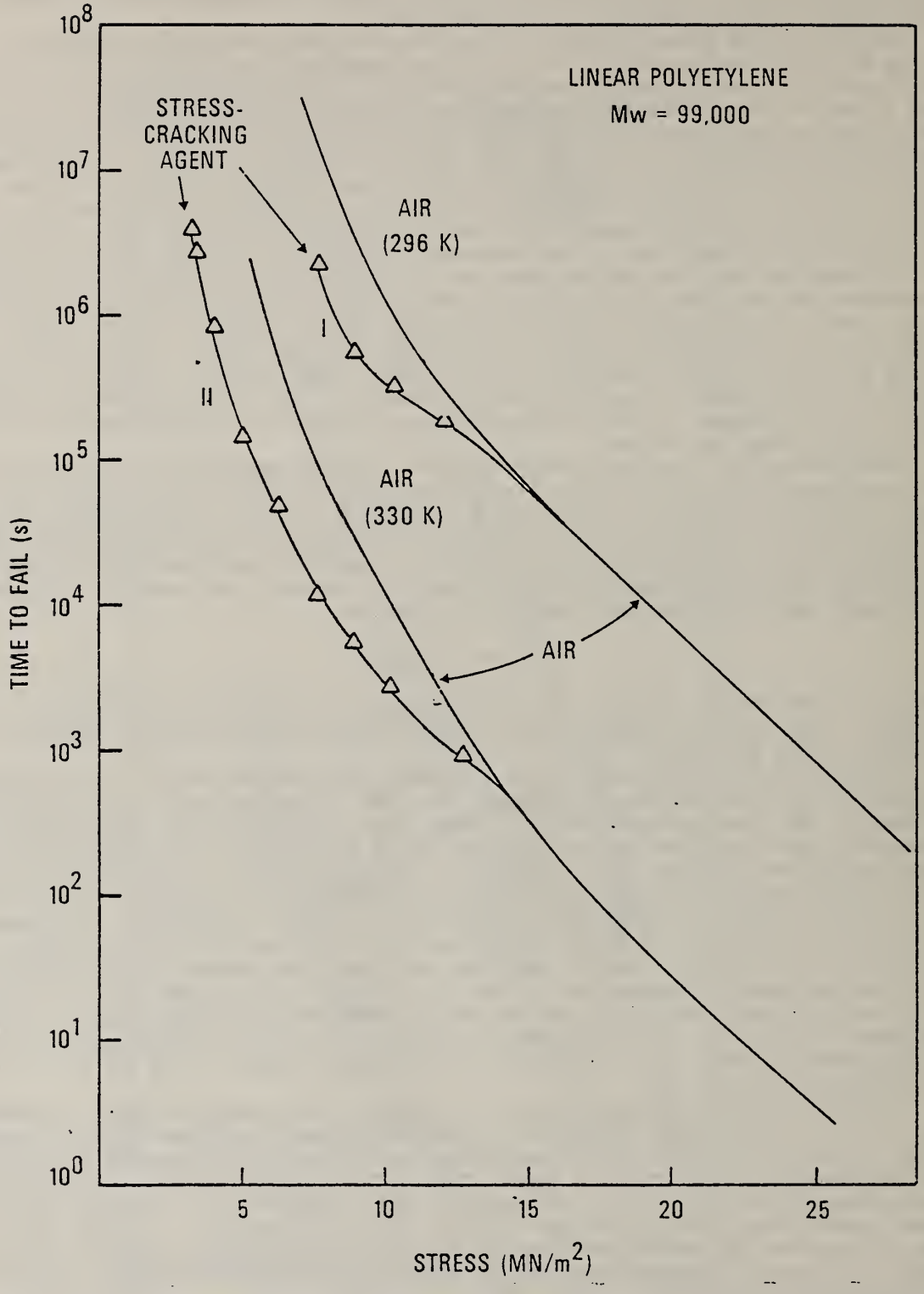

Figure 2.1.5 - Log time to fail versus applied stress in uniaxial creep for high density linear polyethylene (M_W = 99,000) in air (——) and in nonylphenoxypoly(ethleneoxy)ethanol (——△——)

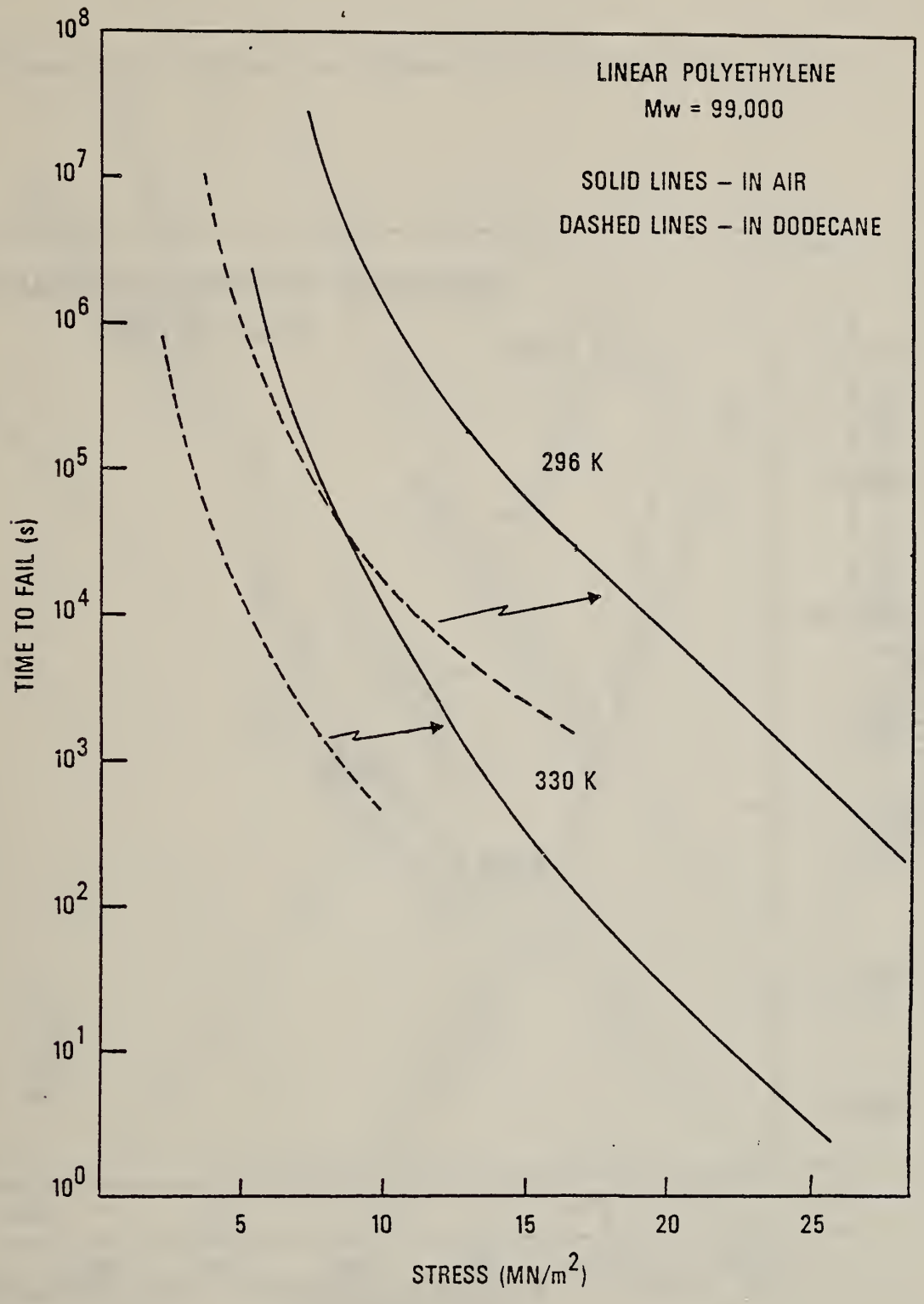

Figure 2.1.6 - Log time to fail versus applied stress in uniaxial creep for high density linear polyethylene in air (——) and in dodecane (----).

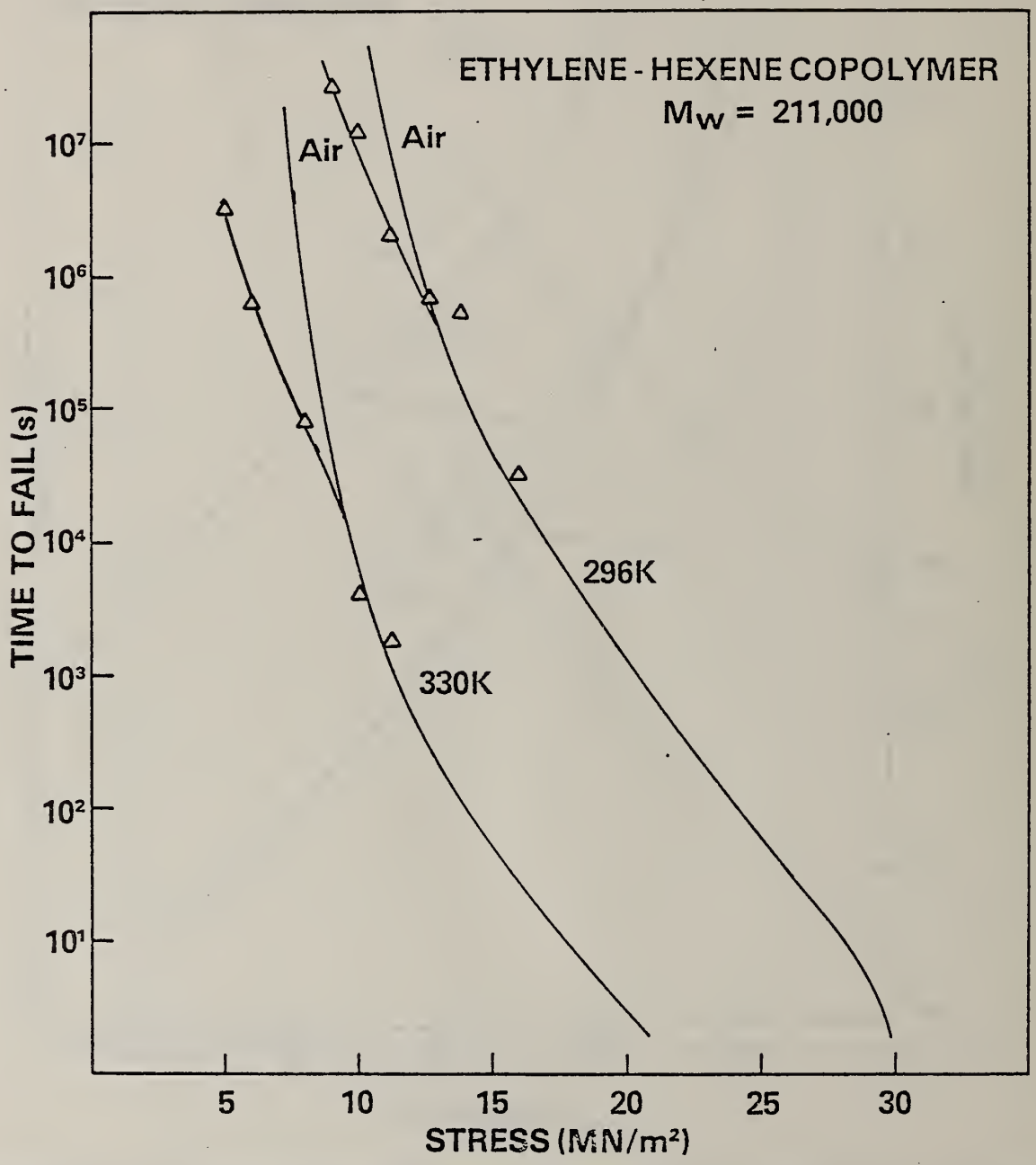

Figure 2.1.7 - Log time to fail versus applied stress in uniaxial creep for an ethylene-hexene copolymer (M_W = 211,000) in air (——) and in nonylphenoxypoly(ethyleneoxy)ethanol (——△——).

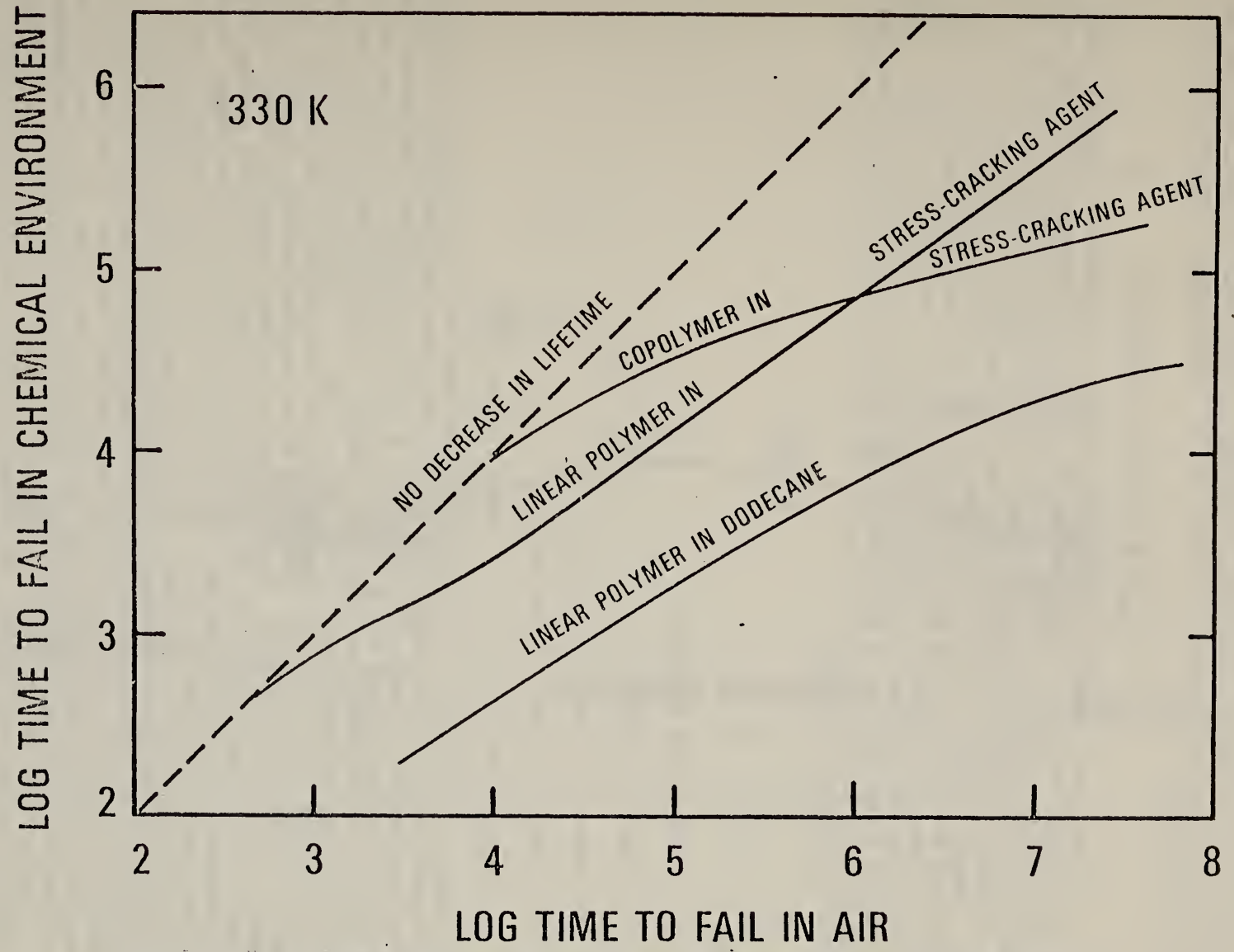

Figure 2.1.8 - Log time to fail in adverse chemical environment versus log time to fail in air for high density linear polyethylene (M_W = 99,000) and an ethylene-hexene copolymer (M_W = 211,000).

becomes greater at longer times than for the linear polyethylene. Yet due to the fact that at small stresses the copolymer experiences a very much longer lifetime in air, for a given stress level, more time is still required for the copolymer to fail in the stress-cracking agent than for the linear polymer. The curve showing the behavior of the linear polymer in dodecane demonstrates that the solvent strongly effects even the early time behavior and that a significant reduction in lifetime occurs over the entire time scale investigated.

2.2 Equal Biaxial Under Inflation

Up to this point we have considered the stress-crack behavior in uniaxial creep. In the next several sections we shall examine the stress-crack behavior of the same two high density polyethylenes under a variety of biaxial deformation histories. The first of these to be considered is one involving equal biaxial deformations induced by inflation. The experimental arrangement has been described in some detail in Section 3.3 of Part III [3]. However, a number of experimental details need to be elaborated on here, so that an abbreviated description of the method will again be given here. The specimen, in the shape of a flat sheet, is clamped at its outer edge as shown in the diagram in Figure 2.2.1. The system is then pressureized at constant internal pressure until failure occurs. Failure is detected either by sound or more often by the feel of escaping gas. For the geometry shown in Figure 2.2.1, an equivalent, or radial, stress can be calculated at the pole of the bubble from the expression

$$\sigma = \frac{Pr\lambda^2}{2h}$$

where

σ = radial stress component

P = internal pressure

r = radius of curvature at the pole

h = initial thickness of the sheet

λ = stretch ratio given by $1 + \varepsilon$, where ε is the strain

The equation is valid only in the vicinity of the pole. and for strains up to about 50%. At distances very far from the pole, or for strains larger than about 50%, the surface no longer approximates a sphere. In cases where a stress-cracking agent was present a small amount of liquid was placed in the bottom of the pressure reservoir, then after pressurization the entire assembly was immediately inverted so that the stress-cracking agent was in contact with the specimen only in its polar region. In the present experiment, the stress-cracking agent was only in contact with the inner surface of the specimen. Had it been in contact with both sides, the results to be described presently may have been different. One difficulty inherent in this method occurs when the applied internal pressure is small (long times to fail). At low pressures the situation can arise whereby the radius of curvature in the specimen becomes smaller in the region of the clamp than at the pole. In this event, the failure may occur preferentially at the clamp, a region for which the stress and strain are not determined. This problem was particularly troublesome when the tests were carried out at high temperature in the presence of stress-cracking agent. At high temperature, water vapor containing the stress-cracking agent was found to preferentially attack the region with convex curvature near the clamp, to the extent that in some cases the specimens cracked almost the entire way around the ring. For this reason, only data for which the failure occurred in the region near the pole will be presented.

The specimens were prepared by compression molding flat sheets 15 cm in diameter and nominally 0.060 cm in thickness. The temperature history during molding was controlled according to the same procedures used to mold the uniaxial specimens. For a given specimen the thickness was determined at several locations within a region 1.5 cm in radius about the center of the sheet. Typically, a variation in thickness of about 0.002 cm was observed, and for purposes of calculating the stress the minimum value recorded was used. From specimen to specimen the minimum thickness varied by up to 0.005 cm. Therefore, in

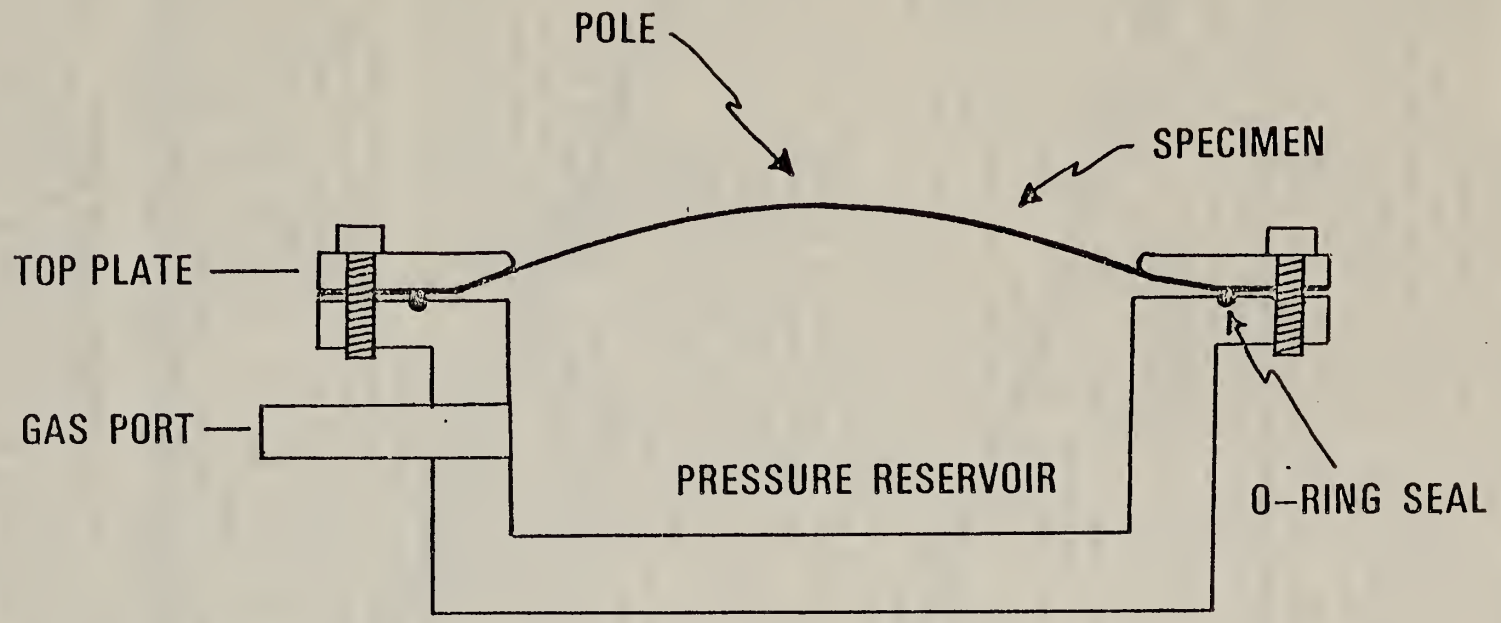

Figure 2.2.1 - Schematic diagram of apparatus for determining stress-cracking behavior under equal biaxial (inflation) deformations.

cases where the data are presented in terms of the applied internal pressure, the values of pressure quoted have been normalized to a constant sheet thickness of 0.060 cm. The strain was determined with the aid of two sets of india ink marks placed at right angles to one another 1.5 cm from the center of the sheet.

Shown in Figure 2.2.2 on log-log coordinates is the radius of curvature (as determined at the pole) versus percent elongation for two different linear polyethylenes and the ethylene-hexene copolymer. The data for the branched material are shown by the triangles in the upper portion of the figure. Measurements were carried out on both linear polymers at three temperatures, 296K, 330K, and 360K (87°C). One interesting feature is that for each polymer type, the behavior can be represented rather well by a unique linear relationship over the wide range of deformation and temperature investigated. The primary difference between the two curves for the linear polyethylene samples is a slight difference in slope. Since the true stress depends on both the radius of curvature and strain, under conditions of a constant internal pressure one can use a master curve of this type to determine either quantity after having measured the other.

The complicated true stress behavior of the linear polyethylene at 296K is shown in Figure 2.2.3 for different values of constant internal pressure. At the highest pressures the stress goes through a minimum and then rises to a high value before failure occurs. This region is the equivalent to that for uniaxial creep where the material experiences an instability and eventually necks. In the equal biaxial case the material also becomes unstable and may cold-draw to some extent before failing by the appearance of a crack. On the other hand, at the low pressures the sheets fail by the appearance of a crack before the material becomes globally unstable. In this region, the true stress decreases monotonically, or tends to level off, up to the point of failure. At the smallest pressures the tendency is again one of the global strain, or true stress, being nearly constant over a high percentage of the total lifetime.

In Figure 2.2.4 are shown results for the time to fail in air and stress-cracking agent (on log coordinates) versus applied pressure for the sample of linear polyethylene with M_W = 99,000. Open symbols denote the behavior in air, and filled symbols that in stress-cracking agent. It should be pointed out that similar measurements carried out on the linear polyethylene having on M_W of 192,000 yield almost identical results, to the extent that both sets of data very nearly superpose. Note that in Figure 2.2.4 the independent variable is applied pressure and not stress. We have already seen that the true stress behavior for this type of biaxial deformation is rather complicated (Figure 2.2.3) and there appears at this point to be no straightforward way to represent all the time to fail data in terms of the true stress. Cold-drawing occurs in the region above about 3 MPa at 296K while cracking takes place in the region below 3 MPa. Unlike the uniaxial creep case, the overall curve representing the time to fail behavior, when represented in terms of applied pressure, does show a distinct break where the change in failure mode occurs. Again, the presence of the stress-cracking agent serves to make the abrupt change more distinct. Note that the action of the stress-cracking agent is one of decreasing the lifetime of the linear polyethylene (and the higher molecular weight linear polyethylene as well) by a factor of about ten.

The behavior of the ethylene-hexene copolymer under inflation is shown in Figure 2.2.5. The curves representing the behavior in air are quite steep, to the extent that at 296K the time required to collect data becomes excessive. A small letter "c" placed next to a data point denoted failure by cracking. The remaining specimens failed by the mechanism of cold-drawing. As can be seen, all of the specimens of this material tested at 296K failed by cold-drawing. However, in the presence of the stress-cracking agent the failure mechanism associated with cracking is made much more emphatic to the extent that it is now quite prominent even at room temperature. As was true for uniaxial extension, the use of stress-cracking agent can be an effective means for separating out the mechanism of failure due to cracking.

In the same manner employed earlier, we compare in Figure 2.2.6 the behavior of the two polyethylenes under inflation by plotting the time to fail in stress-cracking agent versus that in air on log-log coordinates. In the equal biaxial case, the rate at which the lifetime is decreased by the presence of the stress-cracking agent is actually greater for the copolymer over the entire time scale at 296K than for the linear polymer. At 330K, the behavior is reminiscent of the uniaxial case where the two curves cross over. However, in the equal biaxial case, the crossover point occurs nearly one decade earlier in time than for uniaxial extension. We point out, however, that even though the rate at which the lifetime is decreased by the presence of the stress-cracking agent is greater for the copolymer, it still experiences a longer lifetime for a given applied pressure. This is

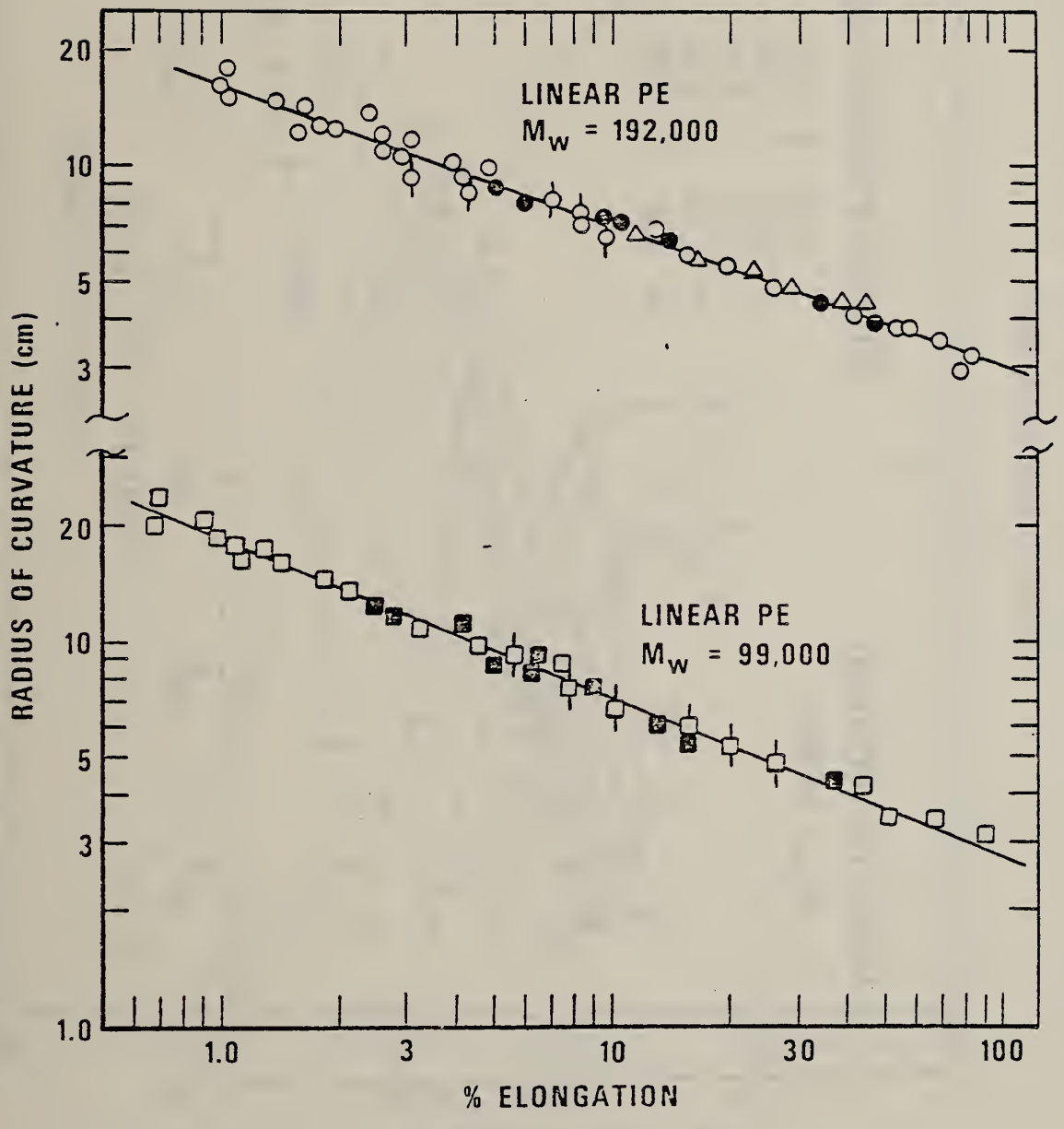

Figure 2.2.2 - Radius of curvature versus percent elongation for polyethylene sheets under inflation. The triangles correspond to the ethylene-hexene copolymer. ○ , □ - 296K; ◍ , ■ - 330K; ◯ , ⊡ - 360K.

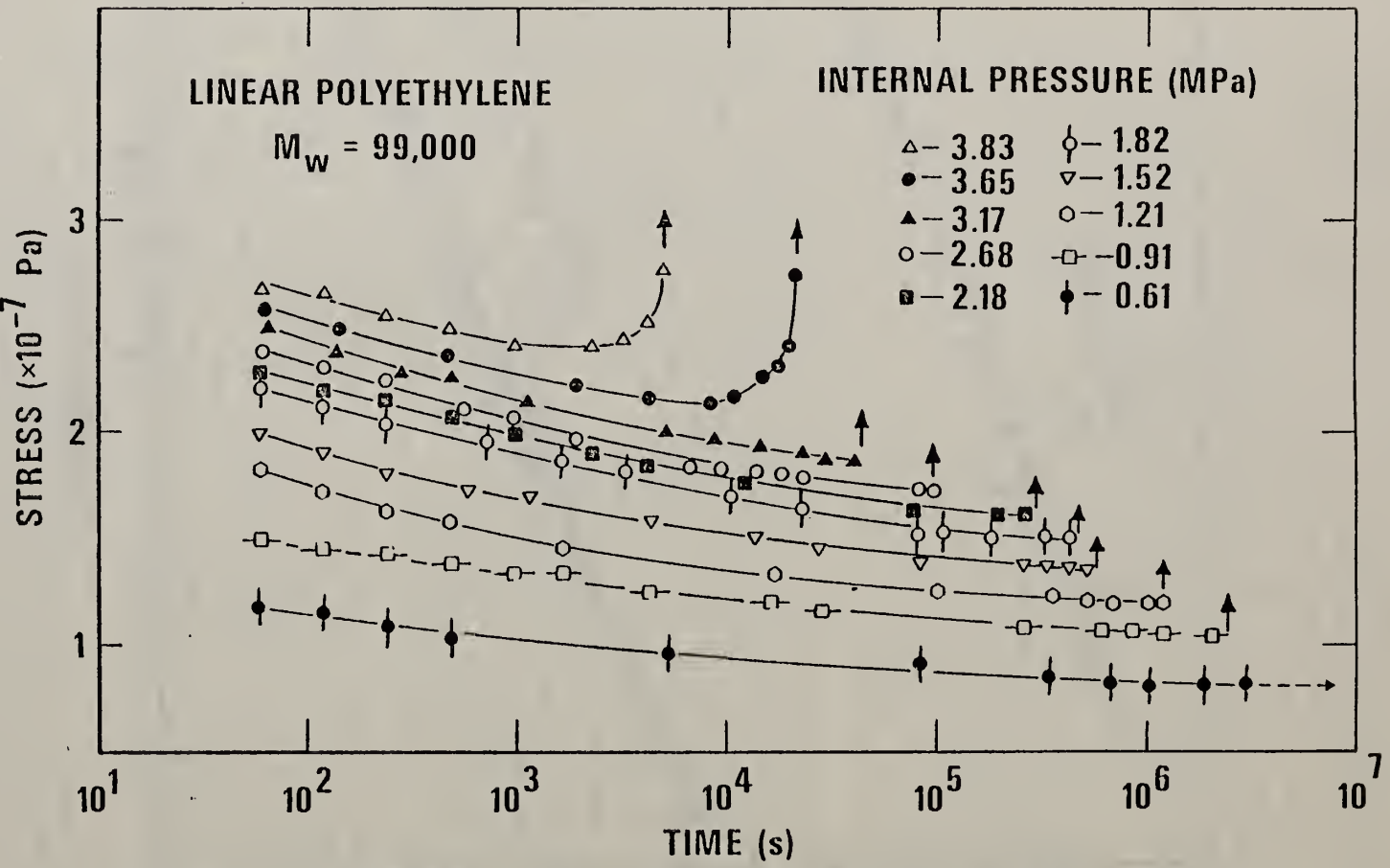

Figure 2.2.3 - True stress versus time for high density linear polyethylene under inflation. The arrows indicate the time at which failure occurred.

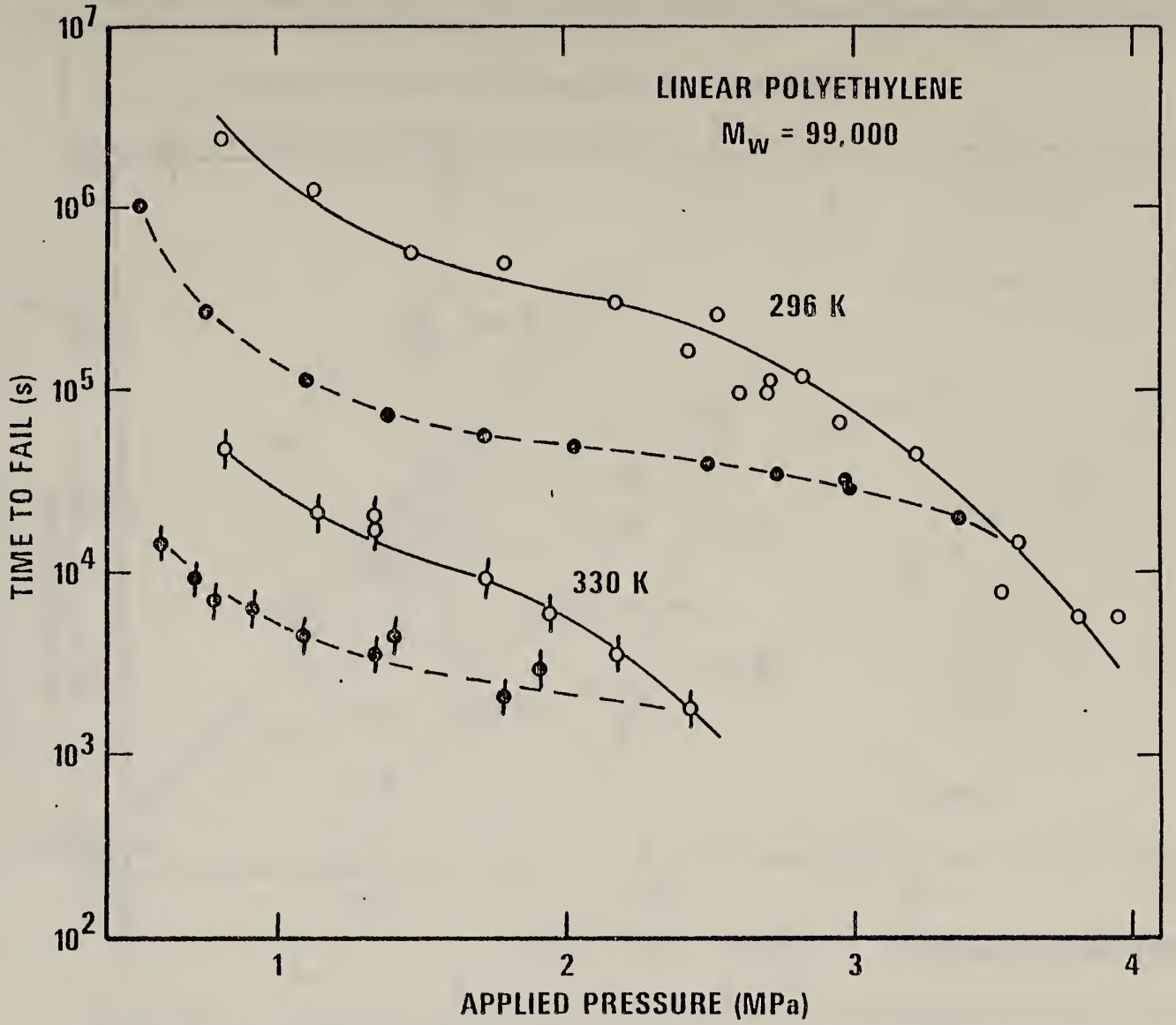

Figure 2.2.4 - Log time to fail versus constant applied pressure for sheets of high density linear polyethylene under inflation in air (○,○) and in nonylphenoxypoly(ethyleneoxy) ethanol (●,●).

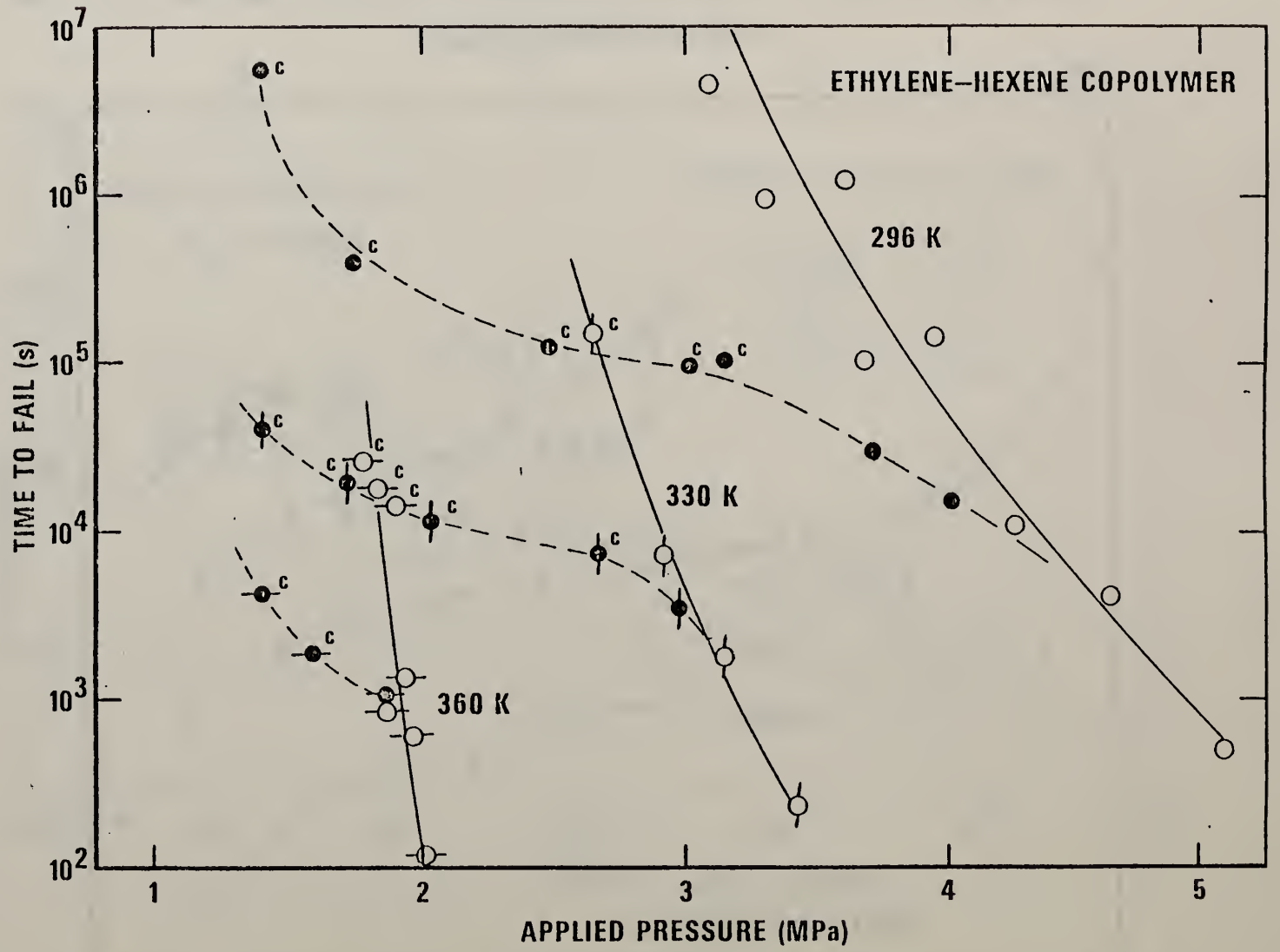

Figure 2.2.5 - Log time to fail versus constant applied pressure for sheets of an ethylene-hexene copolymer under inflation in air (○, ◐, -○) and in nonylphenoxypoly(ethyleneoxy) ethanol (●, ◐, -●).

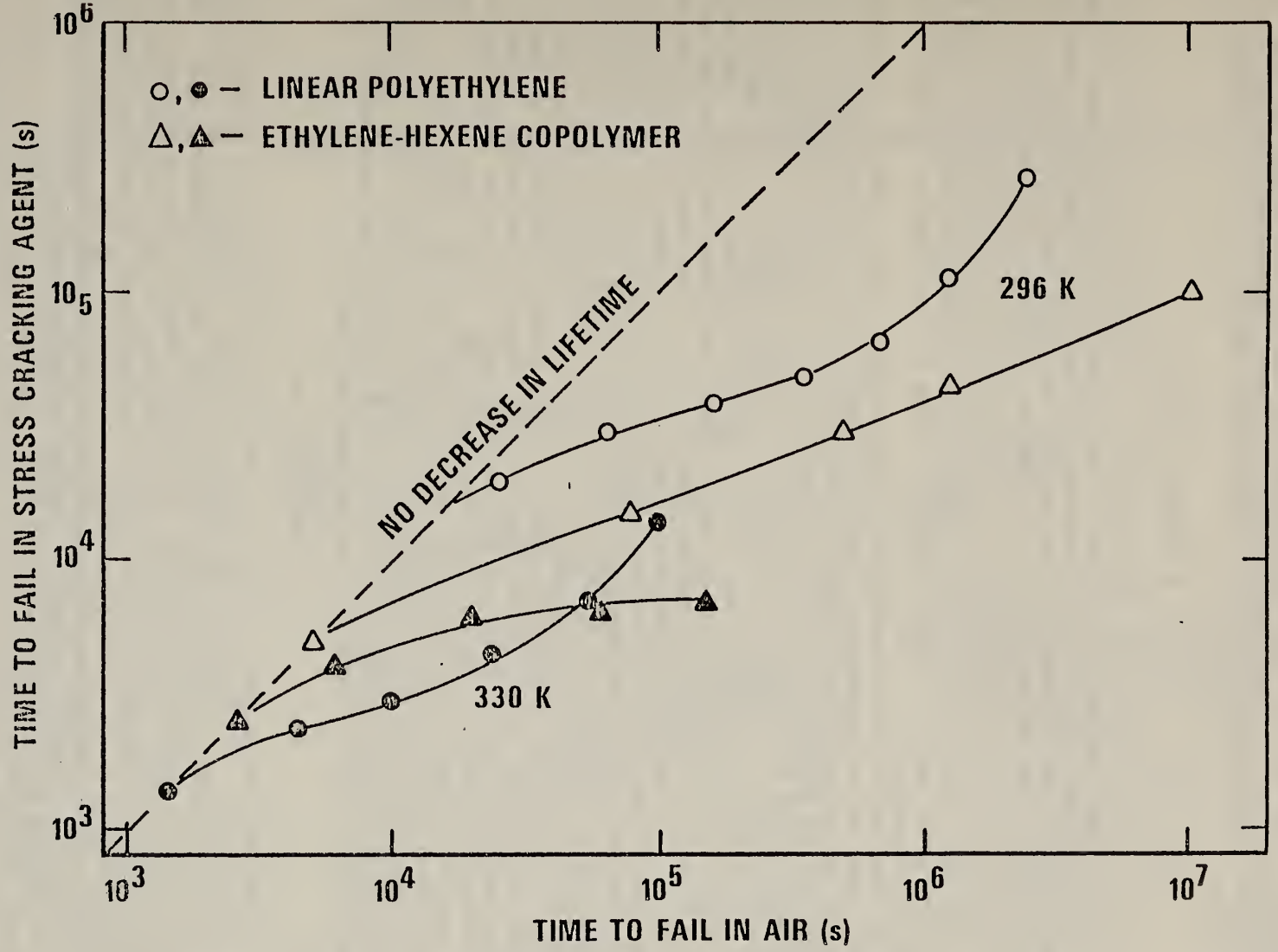

Figure 2.2.6 - Log time to fail in stress-cracking agent versus log time to fail in air for polyethylenes at two different temperatures subjected to equal biaxial deformations under inflation.

because at small pressures the lifetime of the copolymer in air is very much greater than is that of the linear polymer. In fact, if the data from Figures 2.2.4 and 2.2.5 are superposed on one another, it can be seen that for small pressures the lifetime of the copolymer in stress-cracking agent is a factor of ten or more greater than that for the linear polyethylene in stress-cracking agent. It would appear, therefore, that an important factor in determining stress-crack resistance is the ability of the material to perform in air.

2.3 Bottle Inflation

A second type of experiment involving biaxial deformations was bottle inflation at constant internal pressure. This method is reminiscent of ASTM D2561 Standard Method of Test for Environmental Stress-Crack Resistance of Blow-Molded Polyethylene Containers, Procedure C [5]. One difference is that the ASTM test is carried out at one pressure for a period of up to 360 hours, whereas in the present work the bottles were tested to failure at a series of different pressures. In cases where the stress-cracking agent was present, the bottle was partially filled with solution (usually less than 1/4 full) and the bottle then tumbled to insure that initially the entire inner surface was uniformly coated. Time to failure versus applied constant internal pressure data were then collected at three different temperatures.

Our results for 120 ml blow-molded bottles prepared from the same two polyethylenes already described are presented in Figures 2.3.1 and 2.3.2. As was true for uniaxial extension and the equal biaxial under inflation experiment, the failure mode changes depending upon the magnitude of the applied pressure. For the highest pressures employed, the bottles failed by cold-drawing, whereas at the lower pressures failure occurred as a result of cracking. As before, the lifetime of the copolymer bottle in stress-cracking agent was significantly greater than that of the bottle prepared from the linear polymer.

Bottle inflation differs from the bubble type of test described in the last section in that no portion of the bottle deforms equal biaxially. For example, in the region of the side wall of the bottle the material creeps in such a way that the circumference increases with time, while in the direction parallel to the length of the bottle very little deformation occurs. One interesting effect appeared with regard to the particular bottles used in this work. In Figure 2.3.1, consider the data showing the behavior of the linear polymer in stress-cracking agent (filled symbols). Although these bottles failed by cracking, the position in the bottle where the crack appeared depended on the magnitude of the applied pressure. At the higher pressures, the crack occurred in the side wall of the bottle, generally along or close to a mold parting line. This was the same region of the bottle where failure due to cold-drawing occurred at still higher pressures. For the bottles used in this work, this location on the bottle was also the thinnest point. However, at the lowest pressure investigated (at a given temperature) the crack occurred at the chime of the bottle where the curvature and thickness were greatest. This observation underscores the need to examine the stress-crack resustance of the entire container in instances where internal pressure is an important consideration.

2.4 Bent Strip Test

In this section, we shall consider a third type of experiment, one which employs a bent strip geometry. A diagram of the apparatus is given in Figure 2.4.1. The specimen, in the form of a strip, is bent around a metal cylinder and is clamped as shown. The metal cylinder is anchored to a base and the clamp is connected via two pulleys to an applied constant load. The diameter of the cylinder was 1.11 cm (7/16") and the thickness of the specimen was nominally 0.10 cm (0.04"). In cases where the tests were conducted in stress-cracking agent, the specimen assembly was submerged in the liquid maintained at 330K (57°C). Since the failure always occurs in the region of the specimen in contact with the cylinder, there is no need to submerge the specimen completely.

Preliminary results obtained for the linear polymer, both in air and in stress-cracking agent, are shown in Figure 2.4.2. Also included for comparison purposes are the data obtained for the same material in uniaxial creep. The non-homogeneous deformation introduced into the specimen simply by bending it around the cylinder has a pronounced effect on the behavior at loads below about 7.5 MPa, both in air and stress-cracking agent. Note, however, that as the load is increased, the behavior of the bent strip becomes increasingly like that of the uniaxial specimen. Also, it can be seen that even for a condition of zero applied load the bent strip specimens fail within a relatively short time. Under

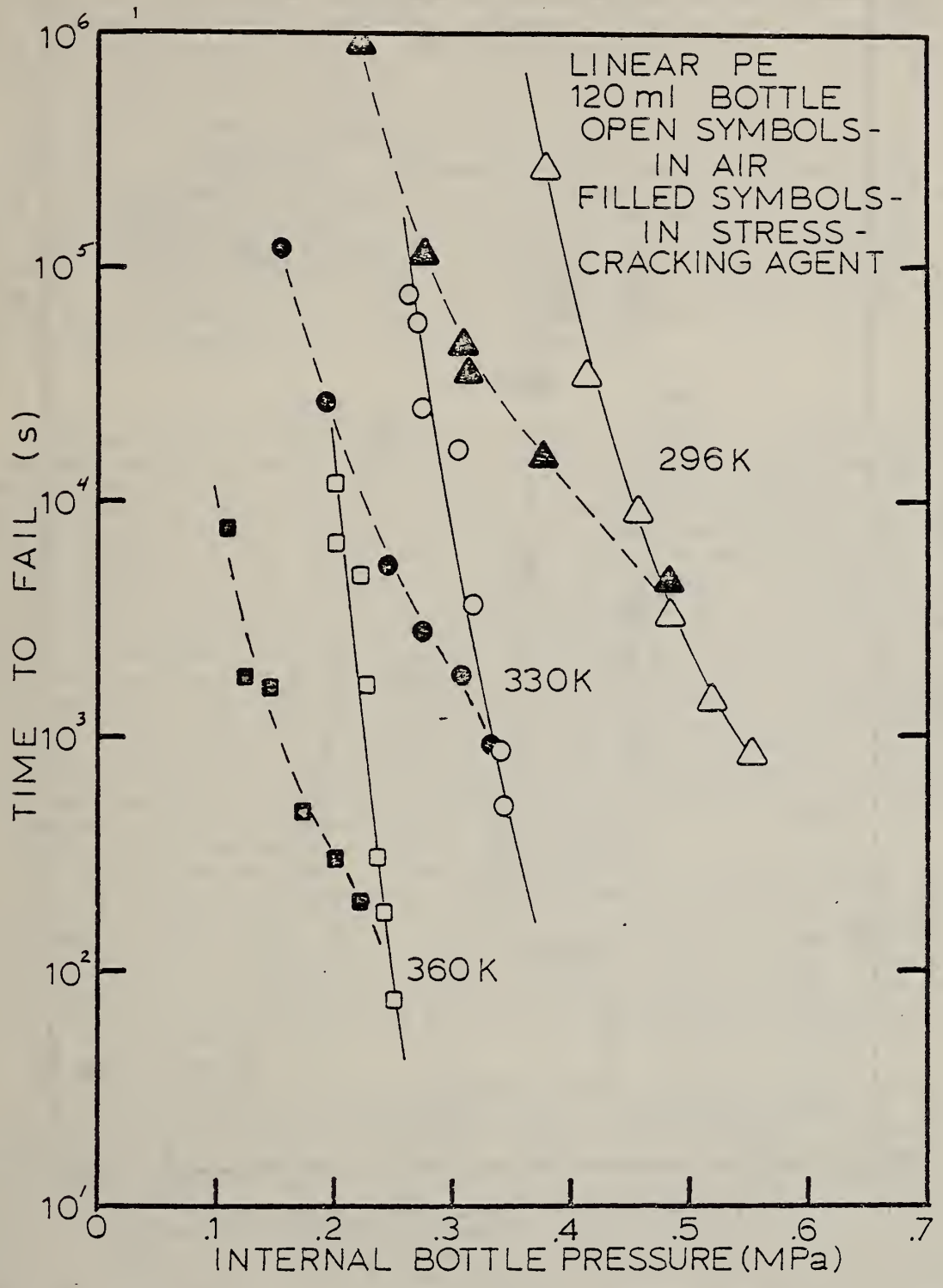

Figure 2.3.1 - Log time to fail versus internal bottle pressure for bottles of high density linear polyethylene (M_W = 99,000) tested to failure under inflation in air and in stress-cracking agent.

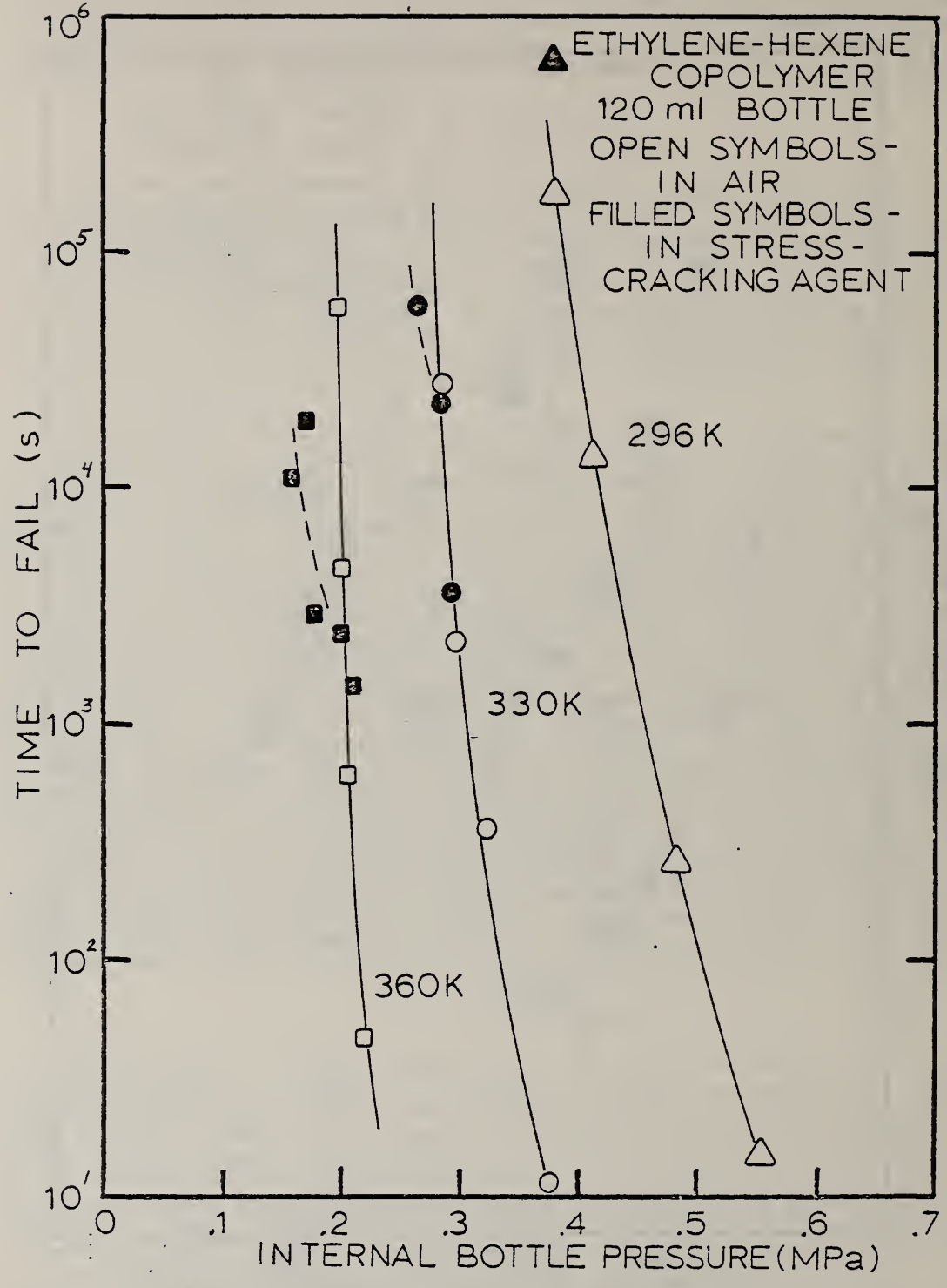

Figure 2.3.2 - Log time to fail versus internal bottle pressure for bottles of an ethylene-hexene copolymer (M_W = 211,000) tested to failure under inflation in air and in stress-cracking agent.

zero applied load, the times to fail in stress-cracking agent are, on average, not greatly different than those quoted by the resin manufacturer for specimens of the same polymer tested according to ASTM D1693 Standard Method of Test for Environmental Stress-Cracking of Ethylene Plastics, Condition A (F_{50} = 15-20 hours) [5]. In the limit of zero applied load, the primary difference between the two methods reduces to one of degree of severity in the bent portion of the specimen, and a notched specimen is used. Also, it should be pointed out that the ASTM test is conducted at 323K (50°C) rather than at 330K (57°C) as was the case here.

The extent to which failure is accelerated by bending the specimen can be controlled to a degree by changing three parameters: the diameter of the cylinder, specimen thickness, and magnitude of the applied load. For example, the thinner the specimen is made or the larger the diameter of the cylinder, the closer the behavior will be to that for uniaxial creep. For specimens which were only one half the nominal thickness of 0.10 cm a significant bending up of the failure curve was observed from that shown in Figure 2.4.2. Also, the scatter in the data becomes decidedly worse as the zero applied load condition is approached. Therefore, it would appear that one advantage to the use of an applied constant load is improved reproducibility. The second obvious advantage is one of time savings in that the time required to produce failure can be reduced.

2.5 Summary

In the manufacture of large polyethylene shipping containers, a test for environmental stress-crack resistance can be useful at one or more stages of production. Prior to processing, such a test provides both a means for screening raw materials and as a quality control measure, for monitoring batch to batch differences in the polymer resin. Following fabrication, the test method may be used to establish performance characteristics of the finished container. In the latter case, the test involves either the cutting of specimens directly from the container and subjecting of them to a stress-crack resistance test such as ASTM D1693 [5], or the container as a whole is subjected to some type of accelerated holding test. Tests carried out on specimens cut from the side wall or ends of the container yield valuable information concerning the effects of processing on the material behavior of those protions of the container. However, because of complicated geometry and/or conditions of processing, the behavior of such specimens may not reflect completely the behavior of the container as a whole. It was noted in Section 2.4 that bottles tested to failure under inflation in a stress-cracking agent failed at different locations on the bottle depending upon the magnitude of the internal pressure. Therefore, testing of the entire container under conditions of varied pressure and temperature may be important. For this purpose, a test of the type described in ASTM D2561 [5] can be applied, since in principle it can be adapted to any size or shape container.

In the work just described, we have investigated the stress-crack behavior of two high density polyethylenes under four different deformation histories. These included uniaxial creep, equal biaxial under inflation, bottle inflation, and bent strip geometries. An important observation was that all four methods yield essentially the same information regarding stress-crack resistance. Another point made is that a primary factor in determining stress-crack resistance appears to be the ability of the material to perform in air, and not necessarily the rate at which failure is accelerated by the stress-cracking agent relative to the behavior in air. Finally, we note that unnotched specimens were used in all four methods examined.

As a test method, uniaxial creep represents a well controlled, easy to perform, experiment, but long testing times are required to obtain the desired information. A test employing equal biaxial deformations under inflation greatly emphasizes the failure mechanism associated with crack growth, and is, therefore, a highly sensitive measure of stress-crack resistance. However, disadvantages are (1) flat sheets of material are required, (2) the state of stress in the specimen as a function of position and time is complex, and (3) the specimens do not always fail in the polar region, especially at elevated temperatures, and the results may tend to be biased. Bottle tests are useful in cases where the geometry of the finished product is suitable for inflation. This type of test is valuable for determining the weakest point. However, the test should probably be carried out at more than one pressure, since it has been demonstrated that in the presence of a stress-cracking agent, the location of the failure can vary with the pressure.

As a general test method for determining environmental stress-crack resistance, the method involving a bent strip geometry described in Section 2.4 appears to combine several of the more desirable features of the various other tests investigated. The experiment is

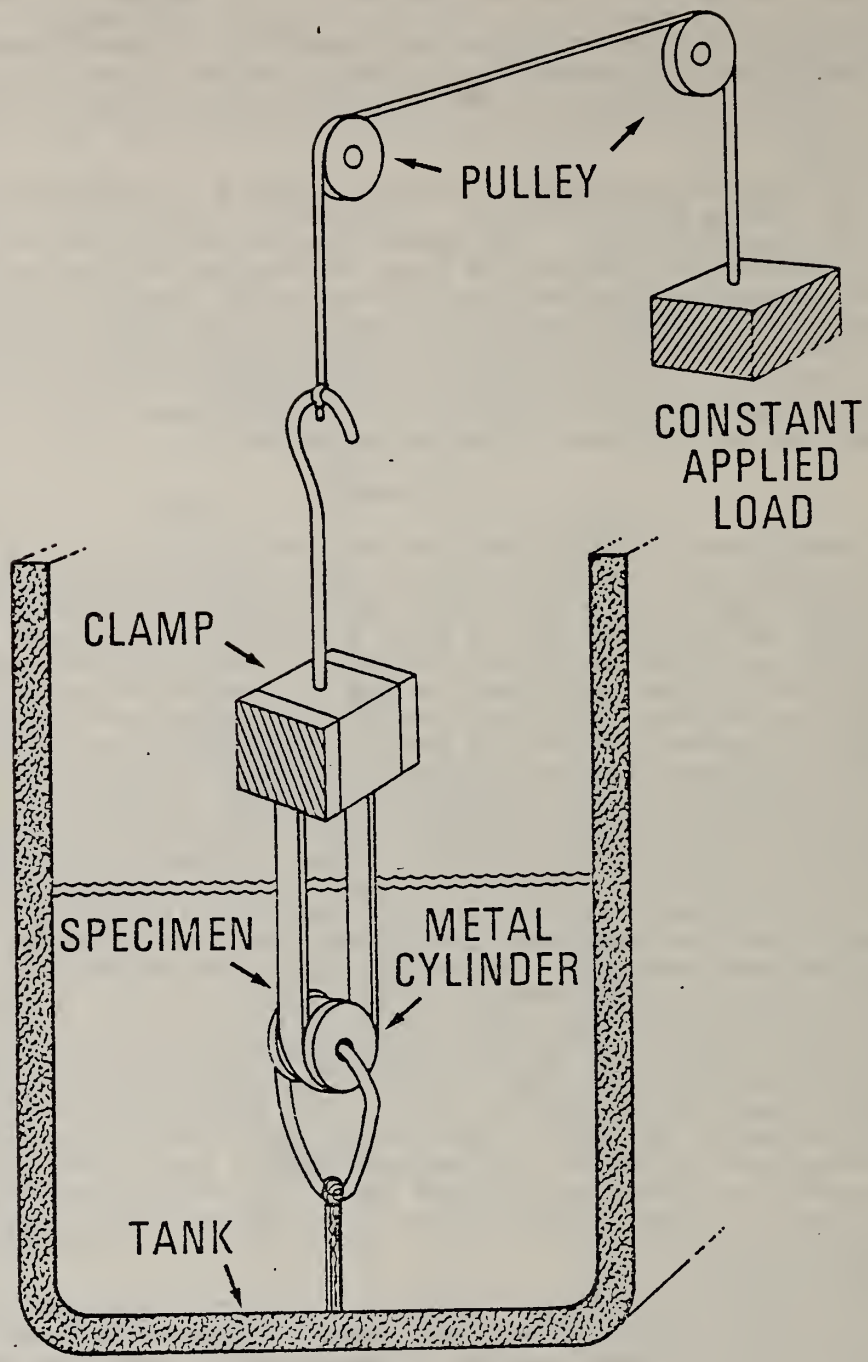

Figure 2.4.1 - Schematic diagram of apparatus for determining stress-crack resistance under conditions of a bent strip geometry with added constant load.

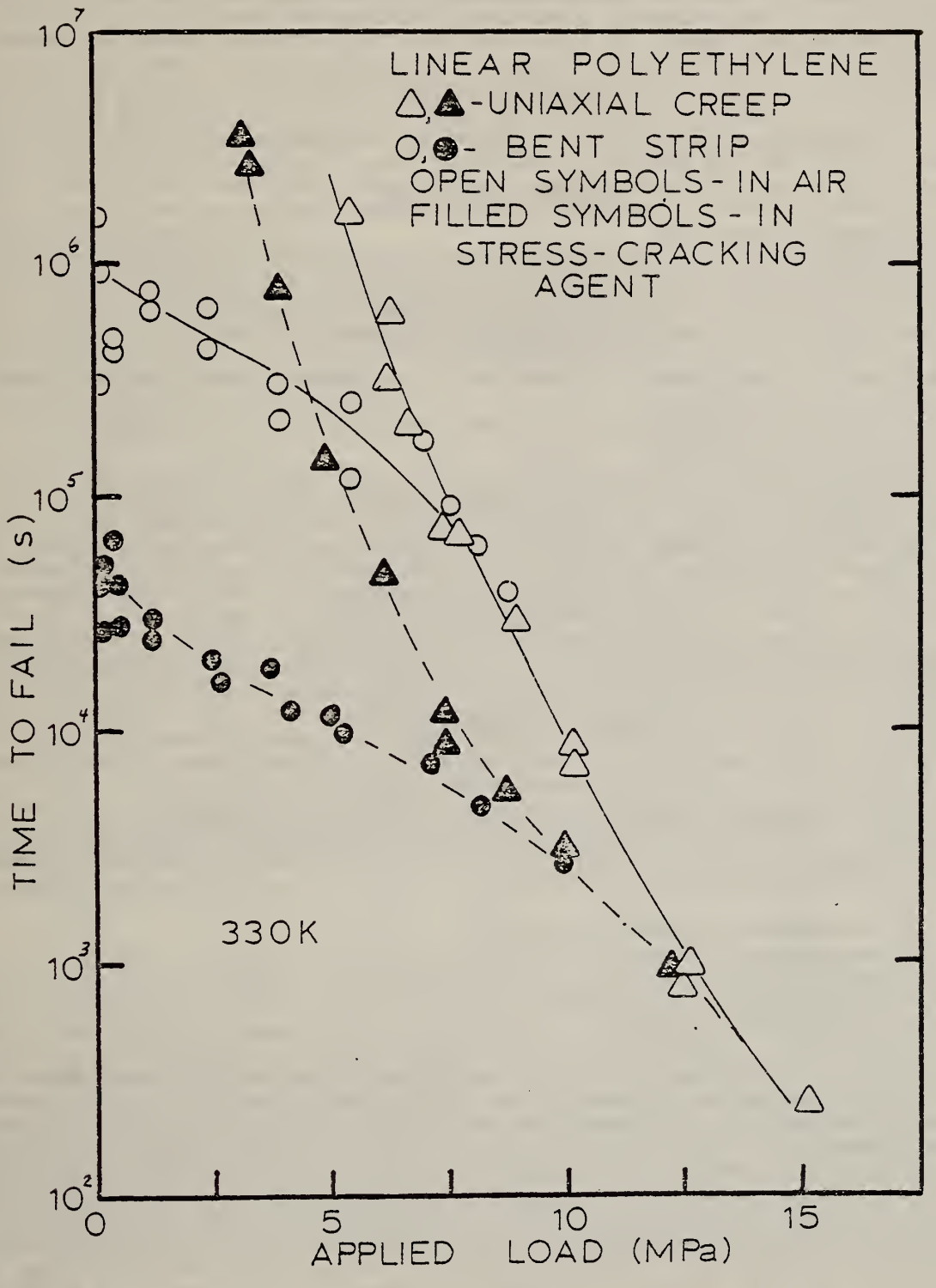

Figure 2.4.2 - Log time to fail versus applied load for specimens of high density linear polyethylene tested to failure in air (O,Δ) and in nonylphenoxypoly(ethyleneoxy)ethanol (●,▲). The circles correspond to the bent strip geometry, the triangles to uniaxial creep.

easier to perform and involves a less complicated state of stress than does the equal biaxial deformation under inflation experiment. At the same time, the bent strip geometry can significantly reduce testing times compared to that required for uniaxial creep tests. Based on preliminary results, it is our view that this particular method has several advantages over the bent strip test currently in widespread use. Under conditions of an uncontrolled bend geometry, the deformation in the region of the bend can be quite severe. As a function of time, the severity of the bend will be influenced by the ability of the specimen to relax, which, in turn, will depend on such factors as crystallinity. In the present method, the bend geometry is controlled for all specimens and constant in time. The imposition of a small constant applied stress appears to have two effects, one of reducing the experimental scatter in the data, and the other of accelerating the failure and thus reducing testing time.

The type of test under consideration here is most suited to situations where the specimens can either be specially molded or cut directly from the processed part. With reference to large shipping containers, this means the machining of specimens either from the side wall or the ends. However, as noted earlier, because of complex container geometry and/or conditions of processing, testing of the entire container under inflation may also be important. The most complete information can be gained by conducting both types of test.

3. Crosslinkable Polyethylene Resins for Rotational Molding

Several years ago, a new class of crosslinkable polyethylene resins for rotational molding entered the marketplace. Such materials are currently coming under the scrutiny of the DoT OHMO as a result of requests for special exemptions for their use in the area of fabrication of large shipping containers for hazardous materials. The rotational molding of crosslinkable polyethylene represents a different approach to container fabrication than that which we shall refer to as "conventional" polyethylene. The physical properties of conventional polyethylene are determined primarily during the manufacture of the polymer resin. Although the processing represents an important step which can influence the performance of the finished product, these properties are determined principally by the polymer chemistry, including factors such as molecular weight distribution, and extent of branching. For crosslinkable polyethylenes, on the otherhand, both the polymer chemistry and physical properties are highly dependent upon the processing, more specifically on the crosslinking step. Properties such as stress-crack resistance, impact strength, and fracture toughness are critically dependent on the degree of crosslinking.

Since the degree of crosslinking clearly represents a key parameter to determining performance characteristics of crosslinkable polyethylene, test methods should be able to directly correlate the two. Several types of test for which it is believed a correlation can be established include the following:

(1) low temperature impact resistance
(2) percentage of extractables
(3) swelling ratio
(4) high temperature tensile modulus
(5) stress-crack resistance

Test number (1) is recommended by a resin manufacturer as a quality control measure to establish a proper degree of crosslinking. The apparent advantage of a test of this type is one of time savings. It also requires very little in the way of costly equipment and can be carried out in the field on specimens of nearly any size or shape. In the absence of quantitative data establishing a correlation between degree of crosslinking and impact resistance, we cannot comment on this test. Tests (2) and (3) are widely used to determine degree of crosslinking and are incorporated into ASTM D2765 Standard Method of Test for Degree of Crosslinking in Ethylene Plastics as Determined by Solvent Extraction [5]. The main criticism of this test is that it requires in excess of 48 hours to perform. Tests (4) and (5) have been suggested as methods which should be highly sensitive to degree of crosslinking. However, based on work described earlier in this report, it must be anticipated that test (5) for stress-crack resistance will be highly time consuming.

In the next several sections we shall summarize experimental work carried out in our laboratory concerned with tests (2) through (4). Experiments concerned with test (5) for stress-crack resistance have been initiated but the work has not yet progressed sufficiently far to be included in this report. For convenient reference, we have included in Table 3.1 a comparison of several material characteristics between crosslinkable polyethylene and

conventional high density polyethylene.

Table 3.1

Comparisoh of Material Characteristics

HDPE	Crosslinkable Polyethylene
Chemical nature	
Linear or lightly branched chains	Crosslinked network
Melt flow properties	
Resin can be characterized by its melt flow index	Melt flow is meaningless
Potential for chemical changes during fabrication	
Limited. Heating, injection, and blow molding cycles are generally relatively short	Substantial. Long cycles at high temperatures are required to distribute the resin and to effect the proper degree of crosslinking
Fabrication process	
Blow molding (in general)	Rotational molding
Applicable ASTM specifications	
D1248 (type III) - Specification for Plastics Molding and Extrusion Materials	D2647 - Specification for Crosslinkable Ethylene Plastics
Nature of Attack by Solvents	
Dissolves	Swells
Recovery at high temperature after plastic deformation	
Partial recovery or melting depending on temperature	Essentially complete recovery

One interesting feature of crosslinkable polyethylene is listed in the last item in Table 3.1, i.e. the ability to recover after large scale deformation. Conventional polyethylenes cold-drawn in uniaxial extension will, when heated to just below the melting point, show partial recovery toward the original configuration. Crosslinkable polyethylenes, on the other hand, can show essentially complete recovery. This is demonstrated in Figure 3.1 for specimens from three different samples of crosslinkable polyethylenes. Characteristics of the three samples are given in the following section. In each case, the specimens labeled A represent the original specimens as cut. Specimens B were subjected to a constant load of 1.23×10^7 Pa and were then allowed to cold-draw in creep to their natural draw ratio ($\lambda \simeq 5$ at 296K). The drawn specimens were then placed in an oven at 423K (150°) for about 2 minutes. The recovered specimens are designated as C. It will be seen in the following section that, based on swell ratio, the three samples have widely different degrees of crosslinking, yet their drawing and recovery behavior is essentially the same.

3.1 Swell Ratio Tests

One of the most widely used tests for establishing degree of crosslinking in polyethylene is a test of the type described in ASTM D2765 Standard Test Method for Degree of

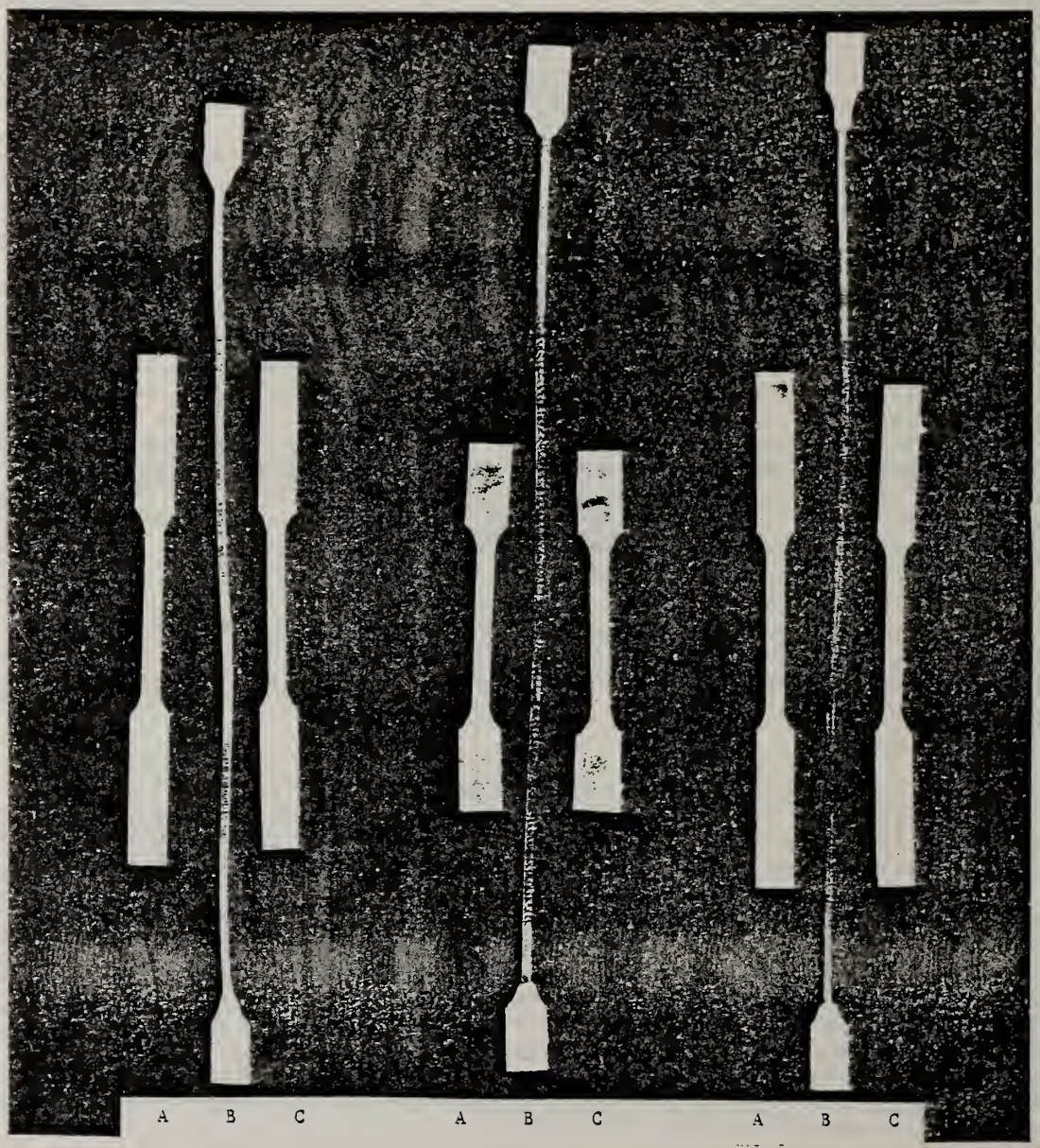

Figure 3.1 - Examples of recovery at elevated temperature after cold-drawing of rotationally molded specimens of crosslinkable polyethylene: A - undeformed specimen, B - cold-drawn specimen, C - recovered specimen after 2 minutes at 423K (150°C).

Crosslinking in Ethylene Plastics as Determined by Solvent Extraction [5]. As noted earlier, this test yields two quantities, the swell ratio and percentage extractables. Both quantities are regarded as representing a measure of degree of crosslinking achieved by the processor. In this section, we shall examine by two different procedures the behavior of eight samples of crosslinked polyethylene. All eight samples were reportedly prepared by the rotational molding technique. Listed in Table 3.1 are the density and percent gel values for each. With the exception of Sample 3, all the samples were obtained from a resin manufacturer who provided the values for percent gel. Gel is the insoluble, non-extractable portion of the resin that is produced by crosslinking. Sample 3 was provided by a commercial fabricator, and the resin was stated to be nominally the same as Sample 1. All density measurements were determined in our laboratory by hydrostatic weighing in distilled water. The error values shown for the density represent an estimate based upon analysis of our measurement technique. It should be observed that, while the density is not a highly sensitive measure of the degree of crosslinking, there is a trend toward higher density with decreased percent gel. This behavior is a likely consequence of greater crystallinity in those samples which are more lightly crosslinked.

Table 3.1.1

Material Properties of Samples Used for Swell Tests

Sample Number	Percent Gel	Density at 296.2K (23.2°C) (g/cm^3)
1	>60	0.941 ± .001
2	>90	0.940 ± .001
3	-	0.940 ± .001
4	50	0.945 ± .001
5	68	0.945 ± .001
6	81	0.942 ± .001
7	82	0.942 ± .001
8	88	0.942 ± .001

Two different types of swell tests were carried out on each sample. In one method, a minimum of three specimens, in most cases four, were cut from different parts of each sample and were tested according to the procedures outlined in ASTM D2765 (Method C). Using this method, both the swell ratio and percentage extractables were determined. In a second set of experiments, a minimum of two specimens were tested as follows. Small rectangular shaped specimens were machined so as to be uniform in dimensions. The length, width, and thickness of each specimen were then measured in the dry state with a micrometer. Each specimen was placed on an aluminum foil tray in a bottle and submerged in xylene to a volume ratio of solvent to specimen of about 500. The bottle, in turn, was placed in a hot oil bath maintained at 383K (110°C) for a period of 24 hours. Consistent with the ASTM procedure, it was found that after 24 hours no further swelling of the specimen occurred. Periodically, the specimens were turned over to insure that no sticking to the foil occurred and to allow each face equal access to solvent. This procedure was found necessary in order to provide uniform test conditions for all materials, since specimens that are lightly crosslinked will creep under their own weight if suspended vertically in the solvent. After 24 hours, the specimen was removed from the xylene and its dimensions measured immediately to the nearest 0.5 millimeter with a ruler. In the event the specimen did not swell uniformly, the dimensions used for the purpose of calculating the swollen volume represent average values. Although no rate of swelling measurements have as yet been performed, one possible advantage of this second type of test is that specimens improperly crosslinked may be sufficiently swollen after only a few hours so as to be considered unacceptable for the intended use.

Results for the two types of swell tests are tabulated in Table 3.1.2. For those specimens tested according to the ASTM procedure both the swell ratio and percent extractables are included. In the case of Sample 4 (50% gel), we were unsuccessful in several attempts to determine a swell ratio based on volume change since the swollen material did not maintain dimensional stability. Therefore, tests based on dimensional changes cannot be expected to be reliable for samples with a percent gel of less than 60%-70%. It is also true that for percent gel levels below 60% the ASTM procedure for determining percent

extractables becomes more difficult since the test procedure relies upon recovering all the non-extractable material from the solvent prior to the drying step. Note that even the most highly crosslinked sample swelled by a factor of ten or more and that about 15% of the material was extracted.

Table 3.1.2

Results of Swell Ratio Tests

Sample	Swell Ratio from ASTM 2765	Percentage Extractable from ASTM 2765	Swell Ratio from Volume Change
	26.1	23.6	
1	26.9	24.5	19.5
	26.9	23.3	19.4
	26.9	23.1	
	12.5	15.7	
2*	12.9	17.4	10.2
	18.0	14.8	11.9
	18.6	15.2	
	51.6	21.3	
	50.0	34.0	
3	49.2	22.3	36.3
	46.3	19.9	41.2
	43.8	25.0	
	40.7	21.4	
	48.4	53.9	
4	44.6	34.9	
	44.7	41.6	
	46.8	56.1	
	44.4	39.8	
5	43.3	36.3	33.9
	44.4	36.7	32.6
	47.0	40.5	
	33.9	26.4	25.9
6	33.4	25.3	24.3
	30.8	24.0	25.2
	31.8	22.9	25.2
	35.0	22.4	30.1
7	34.5	19.8	31.1
	37.7	24.3	34.8

	37.8	23.9	33.6
	32.6	21.4	30.4
8	33.2	21.0	27.3
	34.5	22.5	33.6
			33.8

*Pieces from two different samples

Another pertinent observation regarding the results shown in Table 3.1.2 is that the swell ratio as determined by volume change is, in most cases, significantly less than the value found using ASTM D2765. This result is due, at least in part, to the fact that in ASTM D2765 the swell ratio is defined to be the volume of polymer in the gel plus the volume of absorbed xylene divided by the volume of polymer in the gel, whereas in the test based on dimensional changes the denominator is the sum of both the volume of polymer in the gel plus the volume of polymer that is extractable, that is

$$\text{swell ratio (ASTM)} = \frac{\nu_g + \nu_s}{\nu_g},$$

$$\text{swell ratio (dimensional change)} = \frac{\nu_g + \nu_s}{\nu_g + \nu_e},$$

where $\nu_g + \nu_e$ represent the total initial volume.

In order to examine more closely the correlation between data obtained from the two tests we show in Figure 3.1.1 the swell ratio as determined by ASTM D2765 plotted versus the swell ratio found from dimensional changes. The vertical and horizontal lines with bars represent the spread in values for each sample and the crossover point corresponds to the arithmetic mean for the two directions. The data suggest that there is nearly a linear correlation between the values for swell ratio as determined by the two types of test. Although the number of specimens tested from each sample was too small for any meaningful statistical analysis, we point out that, for the data given in Table 3.1.2, the variances, on average, are smallest for the method employing dimensional changes and largest for the percentage extractable measurements. We conclude, therefore, that the determination of the swell ratio by careful measurement of dimensional changes can yield comparable information concerning degree of crosslinking to that obtained with ASTM D2765, and with equal reproducibility.

3.2 High Temperature Tensile Modulus

It has been suggested that the high temperature tensile modulus may be useful as a measure of degree of crosslinking in crosslinked polyethylenes. Such a test would have appeal from the viewpoint of time required to perform the test compared to swell tests. In both conventional and crosslinked polyethylene the tensile properties are determined in large measure by the crystallinity, the more crystalline the material the higher the tensile modulus. At temperatures below the melting point, the tensile modulus will be rather insensitive to changes in degree of crosslinking. However, at temperatures above the crystalline melting point, the mechanical integrity of the crosslinked material will be maintained solely by the crosslinked network, which does not melt, and it is anticipated that the tensile modulus of the network alone will be sensitive to the extent of crosslinking. The remainder of this section will be concerned with experiments carried out in our laboratory in an effort to determine the feasibility of such a test as a means of establishing degree of crosslinking.

Shown in Table 3.2 are several sample characteristics for sample 1-3 described earlier.

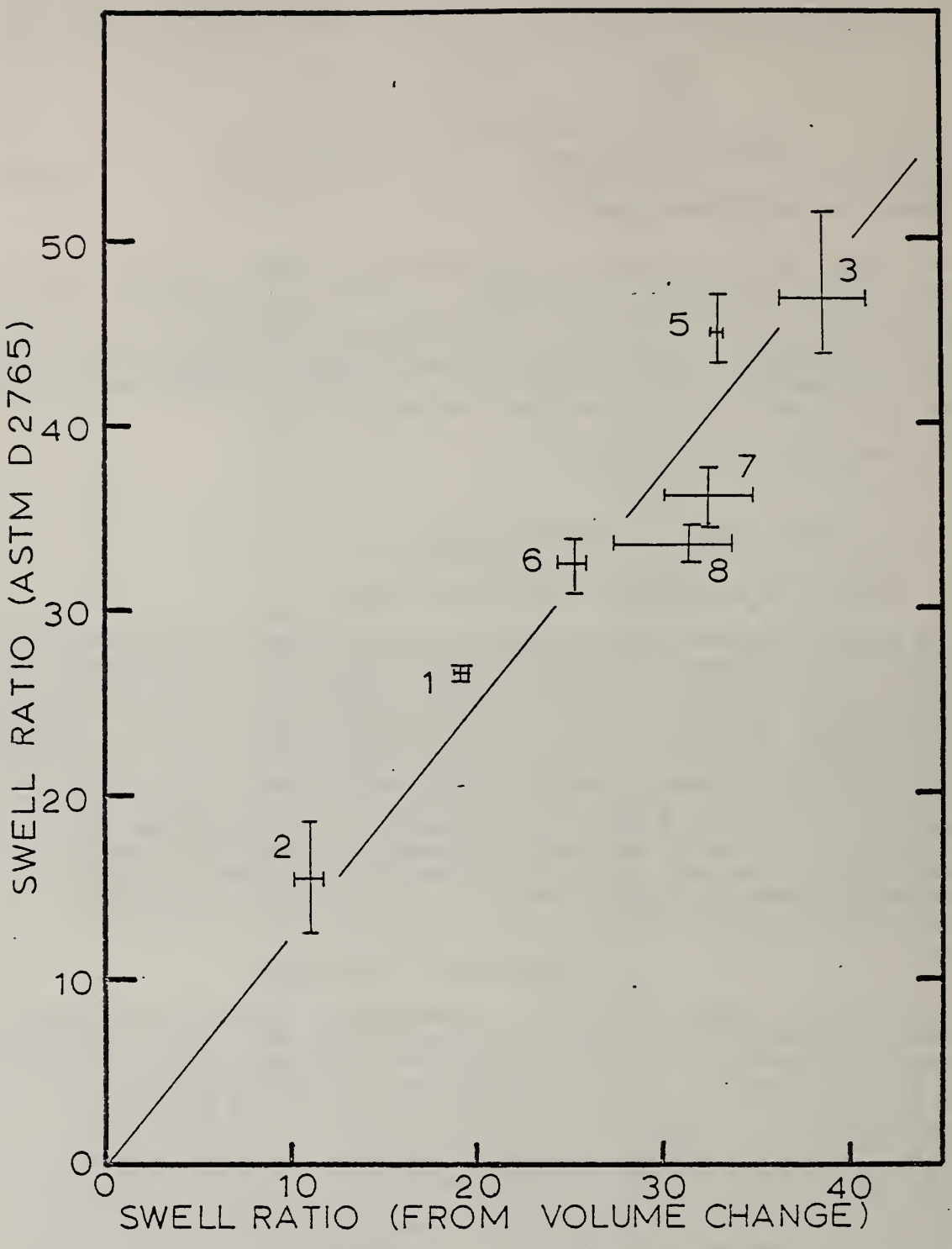

Figure 3.1.1 - Correlation of swell ratio as determined by ASTM D2765 to that determined from dimensional changes for samples of rotationally molded crosslinkable polyethylene having different degree of crosslinking.

Table 3.2

Sample Characteristics of Crosslinked Rotationally Molded Polyethylene

Sample	Density (gm/cm^3)	ESR[3] (hrs.)	Flexural Modulus[4] (kPa)
1	0.937-0.940[1] (0.941)[2]	200	760,000
2	0.930-0.933[1] (0.942)[2]	>1000	690,000
3	0.940[2]	undetermined	undetermined

(1) ASTM D1505 - As determined by resin manufacturer
(2) As determined in our laboratory by hydrostatic weighing - averaging of six specimens
(3) ASTM D1693 Standard Method of Test for Environmental Stress-Cracking of Ethylene Plastics, Condition A - As determined by resin manufacturer
(4) ASTM D790 - As determined by resin manufacturer

In one set of experiments, specimens were prepared by first machining flat sheets from each of the three samples. Dumbbell shaped specimens were then cut from each sheet with a die so that the final dimensions of the straight portion of the specimen were approximately 2.75 cm in length, 0.32 cm in width, and 0.20 cm in thickness. These specimens were then tested to failure in uniaxial creep under static load conditions in a manner identical to that described in Parts I and III of this series of reports [1,3]. To be consistent with terminology used in the previous reports we shall again define failure to be the time at which the specimen either necked or fractured due to cracking, whichever occurred first. Results for these tests are presented in Figure 3.2.1 which shows the time to fail in logarithmic coordinates plotted versus the applied load, all data taken at 296K. As is evident, there is little, if any, difference in behavior for all three samples. It was also true that no significant difference occurred for specimens cut at either 45° or 90° to the direction for which the specimens shown in Figure 3.2.1 were cut. Compared to conventional polyethylenes, the curve shown in Figure 3.2.1 for the crosslinked samples is even steeper than that for the ethylene-hexene copolymer given in Figure 2.1.3. We remarked earlier in this section that the tensile modulus is not likely to depend critically upon the degree of crosslinking at temperatures below the crystalline melting point. It is apparent that the time to fail versus applied load behavior is also insensitive to the degree of crosslinking even though the swelling ratio differs by as much as a factor of four for these three samples.

Next, the tensile modulus (Young's modulus) was determined at 433K (160°C) for specimens taken from samples 2 and 3 described in Table 3.2. Of the three samples, these two exhibited the greatest difference in swelling ratio and presumably, therefore, have the greatest difference in degree of crosslinking. Measurements of the tensile modulus were accomplished with the aid of an Instron Tensile Tester Model 1130* equipped with a 500 gram load cell. In order to carry out the measurements at high temperatures an oven was specially constructed so that both the grips and specimen were well within the controlled temperature zone. Temperature was measured with a temperature transducer device placed as close as possible to, but not touching, the specimen. The temperature gradient over the length of the specimen was determined to be no more than about 2K (2°C). For this set of measurements, the specimens were in the form of straight strips rather than dumbbell shaped as in the time to fail study.

After mounting the specimen in the grips and setting the oven in place, the specimen was slowly heated to 423K (160°C), a temperature well above the highest melting temperature for the crystalline material. Due to thermal expansion of the polymer during heating, particularly through the melting region, some difficulty was encountered in maintaining the specimen in a zero load condition prior to running the test. On our machine, this could be

*Certain commercial materials and equipment are identified in this report in order to specify adequately the experimental procedure. In no case does such identification imply recommendation or endorsement by the National Bureau of Standards, nor does it imply necessarily the best available for the purpose.

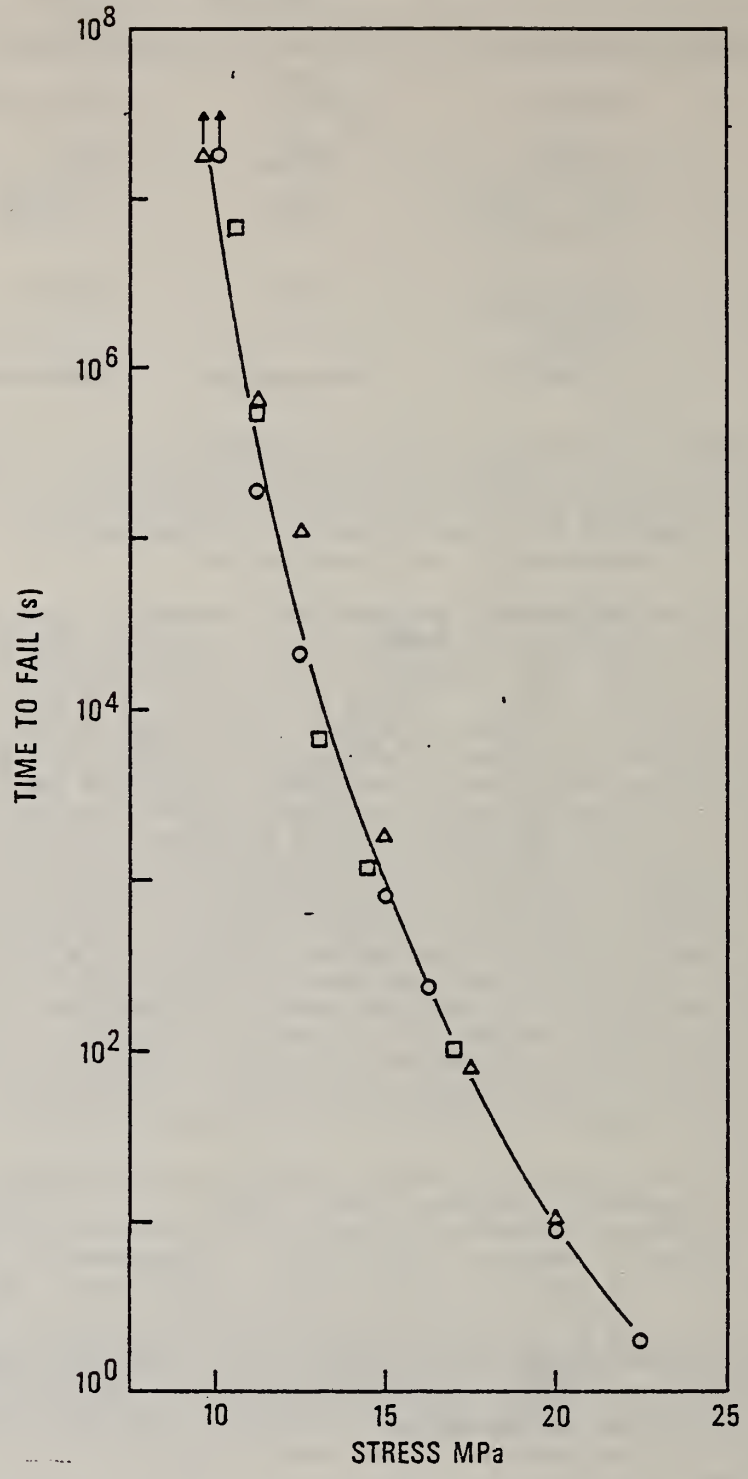

Figure 3.2.1 - Log time to fail versus applied stress for different samples of rotationally molded crosslinkable polyethylene at 296K. △ - Sample 1, □ - Sample 2, ○ - Sample 3.

done only by manual adjustment of the crosshead. This problem would be much less troublesome if the tests were carried out on a machine having a load control capability. Once the specimen had come to temperature equilibrium, the gage length was determined by measurement of the grip separation and the tensile test was then run. The tensile modulus was determined from the initial slope of the stress-strain curve. Ideally, at small deformations, there is a linear portion of the stress-strain curve for which the initial slope represents one measure of the tensile modulus. However, in the present case, the stress-strain curves were nonlinear, even at small deformations, so that it was difficult to determine the initial slope. Therefore, for the type of materials under consideration here, this particular method for determining the tensile modulus must be considered as rather imprecise. For samples 2 and 3, the values obtained for the modulus at 433K by this method were 7.5×10^5 N/m^2 and 5.5×10^5 N/m^2 respectively. Considering the large difference in swelling ratio for these two materials it must be concluded that even the modulus as determined at high temperatures is rather insensitive to the amount of crosslinking.

As a result of the small difference in modulus observed for the two samples, and the high degree of nonlinearity in the stress-strain curve, it was decided to examine these same materials in stress relaxation. The results of this effort are presented in Figure 3.2.2 which shows the stress plotted versus log time for times up to 10^3 seconds ($\approx$ 15 minutes). Also included for comparison are two additional crosslinked materials, one an irradiation crosslinked polyethylene, and a vulcanized natural rubber. The data should not be compared quantitatively since the levels of strain at which the experiments were conducted were not the same for each sample. The point to be made is that all four samples of crosslinked polyethylene show considerable relaxation over the entire time scale covered. In order to properly determine the modulus of the crosslinked network, the stress value should plateau, as it did for the vulcanized rubber after only a few seconds. The plateau region should be sensitive to the degree of crosslinking present. For the four samples of crosslinked polyethylene examined, the stress either will plateau at much longer times than those investigated, or will continue to relax indefinitely. In either case, this type of measurement does not appear practical as a test method, both with regard to sensitivity or time savings.

4. Summary

We have investigated the failure behavior of several types of commercial polyethylene over a wide range of stress and deformation histories, both in air and in stress-cracking agent. It has been shown that the failure mechanism at long times is different from that that short failure times, and, in order to predict long time behavior based on accelerated tests, testing should be done in the region of stress and for deformation appropriate to the failure mode. It has further been demonstrated that a primary factor in determining stress-crack resistance is the ability of the polymer to perform in air, and not necessarily the rate at which failure is accelerated due to the presence of the stress-cracking agent. From the variety of experiments performed (i.e. uniaxial creep, equal biaxial under inflation, bottle inflation, and bent strip geometry) it is apparent that essentially the same information with regard to stress-crack resistance can be obtained from all the methods employed. On this basis we have proposed one possible general test method which combines a number of the more desirable features of the various methods examined, and is a method which we believe has several advantages over ASTM D1693.

In the case of crosslinkable polyethylenes for rotational molding, two possible tests for determining the degree of crosslinking have been examined, tests which might realize a significant time savings over that required to carry out current swell tests. It has been found that a test based on the determination of the high temperature tensile modulus is impractical on several counts. On the other hand, the swell ratio as determined from dimensional changes appears to give an equally reliable measure of the degree of crosslinking as current standard test procedures for determining swell ratio or percent extractables and requires less time to perform. Finally, any activity toward the adoption of test methods such as those developed through this work should be stimulated from within the consensus standards community.

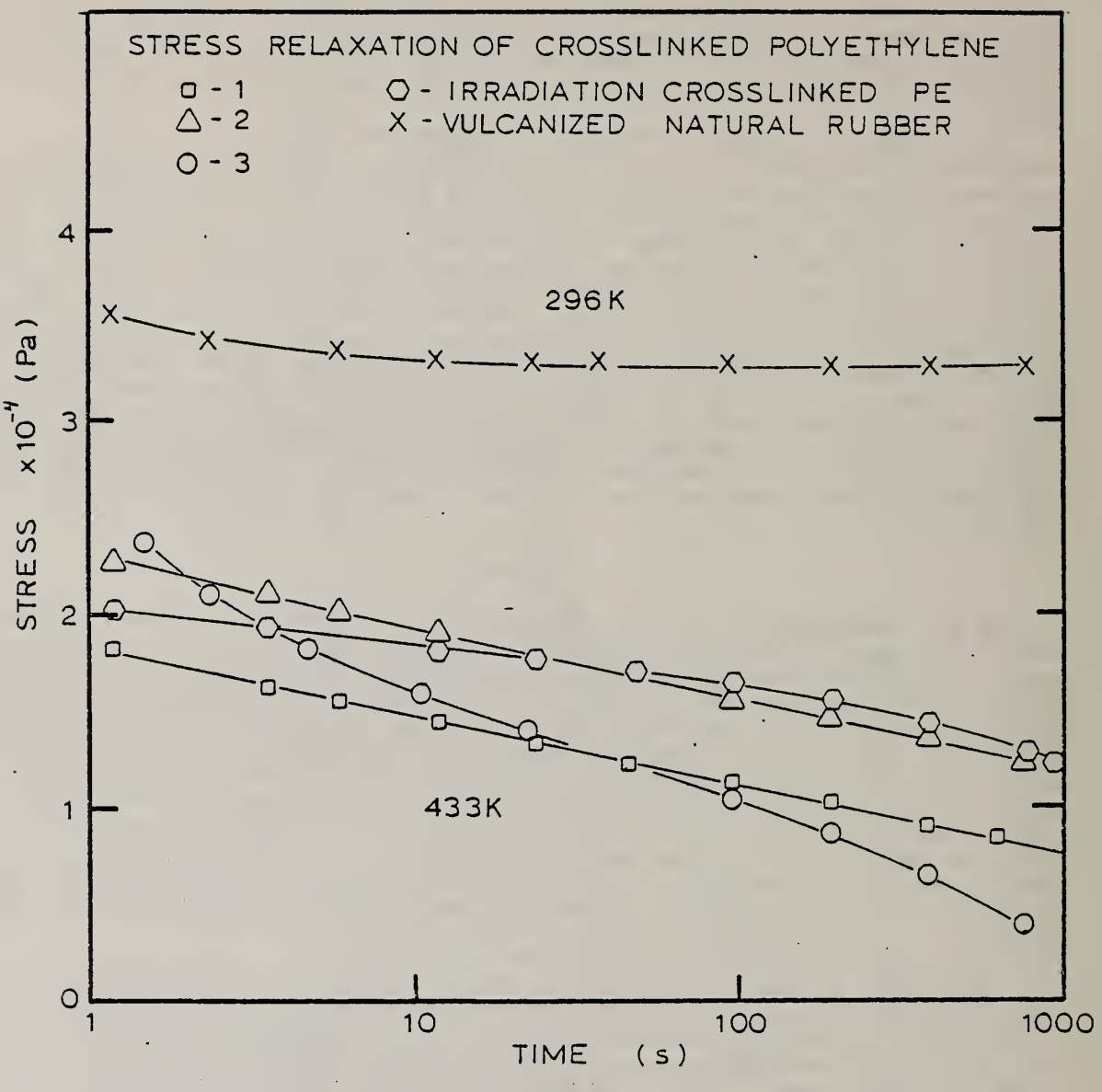

Figure 3.2.2 - Stress relaxation behavior of rotationally molded crosslinked polyethylene.

References

[1] J. M. Crissman, C. M. Guttman, and L. J. Zapas, "Performance of Plastic Packaging for Hazardous Materials Transportation Part I. Mechanical Properties", Report No. DOT/MTB/OHMO-76/4, available from National Technical Information Service, Springfield, VA 22151.

[2] J. D. Barnes and G. M. Martin, "Performance of Plastic Packaging for Hazardous Materials Transportation Part II. Permeation", Report No. DOT/MTB/OHMO-76/5, available from National Technical Information Service, Springfield, VA 22151.

[3] J. M. Crissman and L. J. Zapas, "Performance of Plastic Packaging for Hazardous Materials Transportation Part III. Stress Cracking", Report No. DOT/MTB/OHMO-77/4, available from National Technical Information Service, Springfield, VA 22151.

[4] J. D. Barnes, G. M. Martin, and F. L. McCrackin, "Performance of Plastic Packaging for Hazardous Materials Transportation Part IV. Standardizing Permeation Measurements", Report No. DOT/MTB/OHMO-77/5, available from National Technical Information Service, Springfield, VA 22151.

[5] ASTM 1978 Annual Book of ASTM Standards, Parts 35 and 36, American Society for Testing and Materials, 1916 Race Street, Philadelphia, PA 19103.

[6] Unpublished work.

[7] L. J. Zapas and J. M. Crissman, Polymer Engineering and Science 19, No. 2, 104 (1979).

[8] J. M. Crissman and L. J. Zapas, ACS Symposium Series, No. 95, Durability of Macromolecular Materials, R. K. Eby, Editor, 289 (1979).

[9] J. L. Glathart and F. W. Preston, J. Appl. Phys. 17, 189 (1946).

[10] J. D. Ferry, Viscoelastic Properties of Polymers, Chapter 17, Second Edition, John Wiley and Sons, New York, 1970.

Technical Report Documentation Pag

1. Report No.	2. Government Accession No.	3. Recipient's Catalog No.
DOT/MTB/OHMO-80/2		

4. Title and Subtitle
PERFORMANCE OF PLASTIC PACKAGING FOR HAZARDOUS MATERIALS TRANSPORTATION: PART V MECHANICAL PROPERTIES

5. Report Date
December, 1979

6. Performing Organization Code
NBSIR 79-1938

8. Performing Organization Report No.

7. Author(s)
John M. Crissman, Louis J. Zapas and Gordon M. Martin

9. Performing Organization Name and Address
National Bureau of Standards
U. S. Department of Commerce
Washington, D. C. 20234

10. Work Unit No. (TRAIS)

11. Contract or Grant No.
DOT AS-50074

12. Sponsoring Agency Name and Address
U. S. Department of Transportation
Materials Transportation Bureau
Office of Hazardous Materials Research
Washington, D. C. 20590

13. Type of Report and Period Covered
Final
Oct. 1978 - Oct. 1979

14. Sponsoring Agency Code

15. Supplementary Notes

16. Abstract

This report represents Part V in a series of reports prepared for the U. S. Department of Transportation Office of Hazardous Materials Research under DoT Contract AS-50074. The report summarizes experimental work done in the area of mechanical properties of polymeric materials used in the manufacture of large shipping containers for the transport of hazardous materials. The effort has been directly toward (1) a continuation of studies on the stress-crack resistance of different types of polyethylene, and (2) an examination of various test methods for determining the degree of crosslinking in crosslinkable polyethylenes for rotational molding. The stress-crack resistance of polyethylene has been investigated for four widely different deformation histories, including uniaxial creep, equa biaxial under inflation, bottle inflation, and bent strip geometry. On a basis of information gained from these studies, a test for stress-crack resistance is proposed which combines desirable features from the various methods examined. In the area of crosslinkable polyethylenes, two possible tests for determining degree of crosslinking have been examined. One method involving the determination of the high temperature tensile modulus was found to be impractical, while a swell test based on dimensional changes was found to yield equally reliable results to those obtained by current standard test methods.

17. Key Words	18. Distribution Statement
Crosslinkable polyethylene; failure mechanisms; high temperature tensile modulus; instability under deformation; mechanical properties; polyethylene; stress-crack resistance.	Documentation is available to the U. S. public through the National Technical Information Service, Springfield, VA 22151.

19. Security Classif. (of this report)	20. Security Classif. (of this page)	21. No. of Pages	22. Price
Unclassified	Unclassified	38	

Form DOT F 1700.7 (8-72) Reproduction of completed page authorized